Spectral - Lagrangian methods for Collisional Models of Non - Equilibrium Statistical States

Irene M. Gamba

Dept. of Mathematics & Institute of Computational Engineering and Sciences, University of Texas Austin

Sri Harsha Tharkabhushanam

Institute of Computational Engineering and Sciences, University of Texas Austin

Abstract

We propose a new spectral Lagrangian based deterministic solver for the non-linear Boltzmann Transport Equation (BTE) in d-dimensions for variable hard sphere (VHS) collision kernels with conservative or non-conservative binary interactions. The method is based on symmetries of the Fourier transform of the collision integral, where the complexity in its computation is reduced to a separate integral over the unit sphere S^{d-1}. The conservation of moments is enforced by Lagrangian constraints. The resulting scheme, implemented in free space, is very versatile and adjusts in a very simple manner to several cases that involve energy dissipation due to local micro-reversibility (inelastic interactions) or elastic models of slowing down process. Our simulations are benchmarked with available exact self-similar solutions, exact moment equations and analytical estimates for the homogeneous Boltzmann equation, both for elastic and inelastic VHS interactions. Benchmarking of the simulations involves the selection of a time self-similar rescaling of the numerical distribution function which is performed using the continuous spectrum of the equation for Maxwell molecules as studied first in [13] and generalized to a wide range of related models in [12]. The method also produces accurate results in the case of inelastic diffusive Boltzmann equations for hard spheres (inelastic collisions under thermal bath), where overpopulated non-Gaussian exponential tails have been conjectured in computations by stochastic methods [50; 26; 47; 35] and rigorously proven in [34] and [15].

Key words: Spectral Method, Boltzmann Transport Equation, Conservative/ Non-conservative deterministic Method, Lagrangian optimization, FFT

1 Introduction

In a microscopic description of a rarefied gas, all particles are assumed to be traveling in a straight line with a fixed velocity until they enter into a collision. In such dilute flows, binary collisions are often assumed to be the main mechanism of particle interactions. The statistical effect of such collisions can be modeled by collision terms of the Boltzmann or Enskog transport equation type, where the kinetic dynamics of the gas are subject to the molecular chaos assumption. The nature of these interactions could be elastic, inelastic or coalescing and collision rates may either be isotropic or anisotropic depending on a function of the scattering angle. Usually these interactions are described in terms of inter-particle potentials and their interaction rate is modeled as a product of power laws for the relative speed and the differential cross (angular) section. When such rates are independent of the relative speed, the interaction is called of Maxwell type and when the rates depends on the relative speed they are modeled by a power law with exponents depending on those of the intramolecular potentials and the space dimension as well Rates proportional to positive powers of the relative speed between zero and one are called variable hard potentials interactions, and when the rate is proportional to the relative speed, it is referred to as hard spheres (HS). We point out that the current common taxonomy of particle interactions in the computational physics community denominates variable hard potential interactions by *variable hard sphere* (VHS) interactions. We shall use this nomenclature in the present manuscript.

The Boltzmann transport equation (BTE), or simply stated by the Boltzmann equation, is an integro-differential transport equation that describes the evolution of a single point probability distribution function $f(x, v, t)$ defined as the probability of finding a particle at a position x with a velocity (kinetic) v at a time t. The mathematical and computational difficulties associated to the Boltzmann equation are due to the non local - non linear nature of the integral operator accounting for their interactions. This integral form, called the collision operator, is usually modeled as a multilinear form in d-dimensional velocity space and the unit sphere S^{d-1}, accounting for the velocity interaction law that characterizes the model, as well as by interaction rates as described above.

From the computational point of view, one of the well-known and well-studied methods developed in order to solve this equation is an stochastic based method called "Direct Simulation Monte-Carlo" (DSMC) developed initially by Bird [2] and Nanbu [49] and more recently by Rjasanow and Wagner [55; 56]. This method is usually employed as an alternative to hydrodynamic solvers to model the evolution of moments or hydrodynamic quantities. In particular, this method has been shown to converge to the solution of the classical

Boltzmann equation in the case of monatomic rarefied gases [58]. One of the main drawbacks of such methods is the inherent statistical fluctuations in the numerical results, which become very expensive or unreliable in presence of non-stationary flows or non-equilibrium statistical states. Recent efforts on extensive work done mainly by Rjasanow and Wagner in order to determine from DSMC data the high-velocity tail behavior of the distribution functions can be found in [56] and references therein. Further, implementations for micro irreversible interactions, such as inelastic collisions, have been carefully studied in [35].

In contrast, a deterministic method computes approximations of the probability distribution function using the Boltzmann equation, as well as approximations to the observables like density, momentum, energy, etcetera. There are currently two deterministic approaches to numerically solve the non-linear Boltzmann equation, one is the well-known discrete velocity models and the second a spectral based method, both implemented for simulations of elastic interactions i.e. energy conservative evolution. Discrete velocity models were developed by Broadwell [20] and mathematically studied by Illner, Cabannes, Kawashima among many authors [42; 43; 21]. More recently, these models have been studied for many other applications on kinetic elastic theory in [7; 24; 45; 60; 40]. To the best of our knowledge these approximating techniques have not been adapted to inelastic collisional problems up to this point.

Spectral based models, which are the ones of our choice in this work, have been developed by Pareschi, Gabetta and Toscani [32], and later by Bobylev and Rjasanow [17] and Pareschi and Russo [53]. These methods are supported by the groundbreaking work of Bobylev [4] using the Fourier Transformed Boltzmann equation to analyze its solutions in the case of Maxwell type of interactions. After the introduction of the inelastic Boltzmann equation for Maxwell type interactions and the use of the Fourier transform for its analysis by Bobylev, Carrillo and one of the authors here [6], the spectral based approach is perhaps becoming the most suitable tool to deal with deterministic computations of kinetic models associated with Boltzmann non-linear binary collisional integral, both for elastic or inelastic interactions. More recent implementations of spectral methods for the non-linear Boltzmann equation are due to Bobylev and Rjasanow [19] who developed a method using the Fast Fourier Transform (FFT) for Maxwell type of interactions and then for hard sphere interactions [18] using generalized Radon and X-ray transforms via FFT. Simultaneously, L. Pareschi and B. Perthame [52] developed similar scheme using FFT for Maxwell type of interactions. Later, I. Ibragimov and S. Rjasanow [41] developed a numerical method to solve the space homogeneous Boltzmann equation on a uniform spectral grid for a variable hard shpere interactions with elastic collisions. This particular work has been a great inspiration for our current work and was one of the first initiating steps in the direction of a new numerical method.

We mention that, most recently, Filbet and Russo [27], [28] implemented a method to solve the space inhomogeneous Boltzmann equation using the previously developed spectral methods in [53; 52]. They develop deterministic solvers for non-linear Boltzmann equations have been restricted to elastic interactions. Finally, Mouhot and Pareschi [48] are currently studying the approximation properties of the schemes. Part of the difficulties in their strategy arises from the constraint that the numerical solution has to satisfy conservation of the initial mass. To this end, the authors propose the use of a periodic representation of the distribution function to avoid aliasing and there is no conservation of momentum and energy. Both methods ([28], [27], [48]), which are developed in 2 and 3 dimensions, do not guarantee the positivity of the solution due to the fact that the truncation of the velocity domain combined with the Fourier method makes the distribution function negative at times. This last is a shortcoming of the spectral approach that also is present in our proposed technique. However we are able to handle conservation in a very natural way by means of Lagrange multipliers. We also want to credit an unpublished calculation of V. Panferov and S. Rjasanow [51] who wrote a method to calculate the particle distribution function for inelastic collisions in the case of hard spheres, but there were no numerical results to corroborate the efficiency of the proposed method. Our proposed approach is slightly different that theirs and it takes a less number of operations to compute the collision integral.

Our current approach, based on a modified version from the one in [17] and [41], works for elastic or inelastic collisions and energy dissipative non-linear Boltzmann type models for variable hard shperes. We do not use periodic representations for the distribution function. The only restriction of the current method is that requires the distribution function to be Fourier transformable at any time step. The necessary conservation properties associated to this distribution function are enforced through a Lagrange multiplier constrained optimization problem with the conservation quantities set as the constraints. these corrections, that make the distribution function conservative, are very small but necessary for the accurate evolution of the computed probability distribution function according to the approximated Boltzmann equation.

In addition, the Lagrange optimization problem gives the freedom of not conserving the energy, independently of the collision mechanism, as long as momentum is conserved. Such technique plays a major role as it gives an option for computing energy dissipative solutions by just eliminating one constraint in the corresponding optimization problem. The current method can be easily implemented in any dimension.

A novel aspect of the approach presented here lays on a new method that uses the Fourier Transform as a tool to simplify the computation of the col-

lision operator that works for both elastic and inelastic collisions, which is based on an integral representation of the Fourier Transform of the collision kernel as used in [17]. If N is the number of discretizations in one direction of the velocity domain in d-dimensions, the total number of operations required to compute the collision integral is of the order of $N^{2d}log(N) + O(N^{2d})$. And this number of operations remains the same for elastic or inelastic, isotropic or anisotropic VHS type of interactions. However, when the differential cross section is independent of the scattering angle, the integral representation kernel is further reduced by an exact closed integrated form that is used to save in computational number of operations to $O(N^d log(N))$. This reduction is possible when computing hard spheres in 3-dimensions or Maxwell type models in 2 dimensions. Nevertheless, the method can be employed without many changes for the other case and becomes $O(P^{d-1}\, N^d log(N))$, where P, the number of each angular discretizations is expected to be much smaller than N used for energy discretizations. Such reduction in number of operations was also reported in [28] with $O(Nlog(N))$ number of operations, where the authors are assuming N to be the total number of discretizations in the d-dimensional space (i.e. our N^d and P of order of unity).

Our numerical study is performed for several examples of well-established behavior associated to solutions of energy dissipative space homogeneous collisional models under heating sources that secure existence of stationary states with positive and finite energy. We shall consider heating sources corresponding to randomly heated inelastic particles in a heat bath, with and without friction; elastic or inelastic collisional forms with anti-divergence terms due to dynamically (self-similar) energy scaled solutions [34; 15] and a particularly interesting example of inelastic collisions added to a slow down linear process that can be derived as a weakly coupled heavy and light binary mixture. For this particular case, when Maxwell type interactions are considered, it is shown that [13; 14; 12], on one hand dynamically energy scaled solutions exist, and, for a particular choice of parameters, they have a close, explicit formula in Fourier space, and their corresponding anti Fourier transform in probability space exhibits a singularity at the origin and power law high energy tails, while remaining integrable with finite energy. In addition, they are stable within a large class of initial states. We used this particular example to benchmark our computations by spectral methods by comparing the dynamically scaled computed solutions to the explicit one self-similar one.

Convergence and error results of the spectral Lagrangian method, locally in time, are currently being developed by the authors [36], and it is expected that the proposed spectral approximation of the free space problem will have optimal algorithm complexity using the non-equispaced FFT as obtained by Greengard and Lin [39] for spectral approximation of the free space heat kernel, or self-similar solution of the heat equation. We point out that in our approach the approximation is done by non-equispaced time steps using the

spectral properties of the solution of the problem. This is possible since the self-similar variable is proportional to the quotient of the spectral over time variables, as in the case of the linear heat equation.

Finally we point out that implementations of the space inhomogeneous cases for spacial boundary value problems are also being considered and will be reported in forthcoming work by the authors [37]. The spectral-Lagrangian scheme methodology proposed here can be extended to cases of Pareto tails, opinion dynamics and N player games, where the evolution and asymptotic behavior of probabilities are also well studied in Fourier space [54; 12].

The paper is organized as follows. In the next section we present some preliminaries and description of the various approximated models associated with the elastic or inelastic Boltzmann equation. In section 3, the actual numerical method is discussed with a small discussion on its discretization. We consider in section 4 the special case of the spatially homogeneous collisional model for a slow down process derived from a weakly coupled binary problem with isotropic elastic Maxwell type interactions, where the derivation of explicit solutions for the case of a cold thermostat problem is revisited and shown to have power-like tails. Section 5 deals with the numerical results and examples. Finally in section 6, we discuss and propose directions of future work along with a summary of the proposed numerical method.

2 Preliminaries

The initial value problem associated to the space homogeneous Boltzmann transport equation (BTE) modeling the statistical (kinetic) evolution of a single point probability distribution function $f(v,t)$ for variable hard sphere (VHS) interactions is given by

$$\begin{aligned} \frac{\partial}{\partial t} f(v,t) &= Q(f,f)(v,t) \\ f(v,0) &= f_0(v)\,, \end{aligned} \tag{2.1}$$

In all cases the initial probability distribution $f_0(v)$ is assumed to be integrable. However the problem may or may not have finite initial energy $\mathcal{E}_0 = \int_{\mathbb{R}^d} f_0(v)|v|^2 dv$

The collision or interaction operator $Q(f,f)$ is a bi-linear integral form that can be defined in weak or strong form. The classical Boltzmann formulation is given in strong form is classically given in three space dimensions for hard spheres by

$$Q(f,f)(v,t) = \int_{w\in\mathbb{R}^3,\eta\in S^2} [\frac{1}{'e\,'J} f('v,t)f('w,t) - f(v,t)f(w,t)]\,|u\cdot\eta|\,d\eta dw \tag{2.2}$$

where the integration over the sphere is done with respect to η, the direction the direction that contains the two centers at the time of the interaction, also referred as the impact direction. We denote by $'v$ and $'w$ the pre-collisional velocities corresponding to v and w. In the case of micro-reversible (elastic) collisions one can replace $'v$ and $'w$ with v' and w' respectively in the integral part of (2.1). The exchange of velocities law is given by

$$\begin{aligned} &u = v - w && \text{relative velocity} \\ &v' = v - \frac{1+e}{2}(u\cdot\eta)\eta, && w' = w + \frac{1+e}{2}(u\cdot\eta)\eta\,. \end{aligned} \tag{2.3}$$

This collisional law is equivalent to $u'\cdot\eta = -eu\cdot\eta$ and $u'\wedge\eta = u\wedge\eta$. The parameter $e = e(|u\cdot\eta|) \in [0,1]$ is the restitution coefficient covering the range from sticky to elastic interactions, so $'e = e(|'u\cdot\eta|)$, with $'u$ the pre-collisional relative velocity. The Jacobian $J = |\,\frac{\partial(v',w')}{\partial(v,w)}\,|$ of post-collisional velocities with respect to pre-collisional velocities depends also on the local energy dissipation [22]. In particular, $'J = |\,\frac{\partial('v,'w)}{\partial(v,w)}\,|$. In addition, it can be seen in general that it is a function of the quotient of relative velocities and the restitution coefficient as well. For example and in the particular case of hard spheres interactions

$$J(e(z)) = e(z) + z\,e(z) = (z\,e(z))_z \qquad\qquad \text{with}\quad z = |u\cdot\eta|\,.$$

When $e = 1$ then the collision law is equivalent to specular reflection with respect to the plane containing η, orthogonal to the corresponding tangent plane to the sphere of influence. The direction η is also called the impact direction. We note that $J = 1$ when $e = 1$, that is, for elastic hard sphere interactions. The corresponding weak formulation of the collisional form becomes more transparent and crucial in order to write the inelastic equation in higher dimensions or for more general collision kernels. Such formulation, originally due to Maxwell for the space homogeneous form, and is often call the Maxwell form of the Boltzmann equation. The integration is parametrized in terms of the center of mass and relative velocity, and the on the $n-1$ dimensional spherical integration is done with respect to the unit direction σ given by the elastic post collisional relative velocity, that is

$$\begin{aligned} \int_{v\in\mathbb{R}^d} Q(f,f)(v,t)\,\phi(v)\,dv = \\ \int_{v,w\in\mathbb{R}^{2d},\sigma\in S^{d-1}} f(v,t)f(w,t)[\phi(v') - \phi(v)]\,B(|u|,\mu)\,d\sigma dw dv\,, \end{aligned} \tag{2.4}$$

where the corresponding velocity interaction law is now given by

$$
\begin{aligned}
&v' = v + \frac{\beta}{2}(|u|\sigma - u), \qquad && w' = w - \frac{\beta}{2}(|u|\sigma - u)\,,\\
&u' = (1-\beta)u + \beta|u|\sigma && \text{(inelastic relative velocity)}\,,\\
&\mu = \cos(\theta) \;=\; \frac{u\cdot\sigma}{|u|} && \text{(cosine of the elastic scattering angle)}\,,\\
&B(|u|,\mu) = |u|^{\lambda}\, b(\cos\theta) && \text{with}\;\; 0 \le \lambda \le 1 \quad ,\\
&\omega_{d-2}\int_0^{\pi} b(\cos\theta)\sin^{d-2}\theta d\theta < K \quad \text{(Grad cut-off assumption)}\,,\\
&\beta = \frac{1+e}{2} && \text{(energy dissipation parameter)}\,.
\end{aligned}
\tag{2.5}
$$

We assume the differential cross section function $b(\frac{u\cdot\sigma}{|u|})$ is integrable with respect to the post-collisional specular reflection direction σ in the $d-1$-dimensional sphere, referred to as the *Grad cut-off assumption*, and that $b(\cos\theta)$ is renormalized such that

$$
\begin{aligned}
\int_{S^{d-1}} b(\frac{u\cdot\sigma}{|u|})\, d\sigma \;&=\; \omega_{d-2}\int_0^{\pi} b(\cos\theta)\sin^{d-2}\theta\, d\theta\\
&= \omega_{d-2}\int_{-1}^{1} b(\mu)(1-\mu^2)^{(d-3)/2} d\mu \;= 1\,,
\end{aligned}
\tag{2.6}
$$

where the constant ω_{d-2} is the measure of the $d-2$-dimensional sphere.
The parameter λ regulates the collision frequency as a function of the relative speed $|u|$. It accounts for inter-particle potentials defining the collisional kernel and they are referred to as variable hard spheres (VHS) model whenever $0 < \lambda < 1$, Maxwell molecules type interactions (MM) for $\lambda = 0$ and hard spheres (HS) for $\lambda = 1$.

In the case of elastic hard spheres ($\beta = 1, \lambda = 1$) in 3 dimensions, collision kernel $B(|u|,\mu) = a^2/4$, where a is the particle diameter. For Maxwell type elastic interactions ($\beta = 1, \lambda = 0$), $B(|u|,\mu) = \frac{1}{4\pi} b(\theta)$. For inelastic interactions, even in the case of hard spheres, the angular part of the collision kernel depends on β (see [15]).
For the classical case of elastic collisions, it has been established that the Cauchy problem for the space homogeneous Boltzmann equation has a unique solution in the class of integrable functions with finite energy (i.e. $C^1(L^1_2(\mathbb{R}^d))$), it is regular if initially so, and $f(.,t)$ converges in $L^1_2(\mathbb{R}^d)$ to the Maxwellian distribution $M_{\rho,V,\mathcal{E}}(v)$ associated to the $d+2$ moments of the initial state $f(v,0) = f_0(v) \in L^1_2(\mathbb{R}^d)$. In addition, if the initial state has Maxwellian decay, this property is preserved with the Maxwellian decay globally bounded in time ([33]), and if any derivative of the initial state has a Maxwellian decay,

this behavior will be preserved as well (see [1]).

In all problems under consideration, collisions either conserve density, momentum and energy (elastic), or just density and momentum (inelastic) or density (elastic - linear Boltzmann operator), depending on the number of collision invariants of the operator $Q(f,f)(t,v)$. In the case of the classical Boltzmann equation for rarefied elastic, monatomic gases, the collision invariants are exactly $d+2$, that is, according to the Boltzmann theorem, the number of polynomials in velocity space v that generate $\phi(v) = A + \mathbf{B}\cdot\mathbf{v} + \mathbf{C}|\mathbf{v}|^{\mathbf{2}}$, with $C \leq 0$. In particular, one obtains the following *conserved quantities*

$$\begin{aligned} &\text{density} && \rho(t) &&= \int_{v\in\mathbb{R}^d} f(v,t)dv \ , \\ &\text{momentum} && m(t) &&= \int_{v\in\mathbb{R}^d} vf(v,t)dv \ , \\ &\text{kinetic energy} && \mathcal{E}(t) &&= \frac{1}{2\rho(t)}\int_{v\in\mathbb{R}^d} |v|^2 f(v,t)dv \, . \end{aligned} \tag{2.7}$$

Of significant interest from the statistical view point are the evolutions of moments or observables, at all orders. They are defined by the dynamics of the corresponding time evolution equation for the velocity averages, given by

$$\frac{\partial}{\partial t} M_j(t) \ = \ \frac{\partial}{\partial t}\int_{v\in\mathbb{R}^d} f(v,t)v^{\otimes j}dv \ = \ \int_{v\in\mathbb{R}^d} Q(f,f)(v,t)v^{\otimes j}dv \ , \tag{2.8}$$

where $v^{\otimes j}$ = standard symmetric tensor product of v with itself, j times. Thus, according to (2.7), for the classical elastic Boltzmann equation, the first $d+2$ moments are conserved, meaning, $M_j(t) = M_{0,j} = \int_{v\in\mathbb{R}^d} f_0(v)v^{\otimes j}dv$ for $j = 0, 1$; and $\mathcal{E}(t) = \mathrm{tr}(M_2)(t) = \mathcal{E}_0 = \int_{v\in\mathbb{R}^d} f_0(v)|v|^2 dv$. This can be easily computed from a symmetrized weak formulation (2.4) with test functions which are constant, linear and quadratic of their variable magnitude (these are the so called collision invariants).

Higher order moments or observables of interest are

$$
\begin{aligned}
&\text{Momentum Flow} && M_2(t) \;=\; \int_{\mathbb{R}^d} vv^T f(v,t)dv \;\;, \\
&\text{Energy Flow} && r(t) \;=\; \frac{1}{2\rho(t)}\int_{\mathbb{R}^d} v|v|^2 f(v,t)dv \;\;, \\
&\text{Bulk Velocity} && V(t) \;=\; \frac{m(t)}{\rho(t)} \;\;, \\
&\text{Internal Energy} && E(t) \;=\; \frac{1}{2\rho}(tr(M_2)-\rho|V|^2) \;\;, \\
&\text{Temperature} && T(t) \;=\; \frac{2\mathcal{E}(t)}{\mathbf{k}d} \;\;, \quad \text{with } \mathbf{k} \text{ the Boltzmann constant.}
\end{aligned}
\tag{2.9}
$$

In particular, for the case of Maxwell molecules ($\lambda = 0$), it is possible to write recursion formulas for higher order moments of all orders ([5] for the elastic case, and [6] in the inelastic case) which, in the case of isotropic solutions depending only on $|v|^2/2$, take the form

$$
\begin{aligned}
m_n(t) \;&=\; \int_{\mathbb{R}^d} |v|^{2n} f(v,t)dv = \; e^{-\lambda_n t} m_n(0) + \\
&\sum_{k=1}^{n-1} \frac{1}{2(n+1)} \binom{2n+2}{2k+1} B_\beta(k,n-k) \int_0^t m_k(\tau)\, m_{n-k}(\tau)\, e^{-\lambda_n(t-\tau)}\, d\tau \,; \\
&\text{with} \\
&\lambda_n = 1 - \frac{1}{n+1}[\beta^{2n} + \sum_{k=0}^{n}(1-\beta)^{2k}] \,, \\
&B_\beta(k,n-k) \;=\; \beta^{2k}\int_0^1 s^k(1-\beta(2-\beta)s)^{n-k} ds \,,
\end{aligned}
\tag{2.10}
$$

for $n \geq 1,\ 0 \leq \beta \leq 1$, where $\lambda_0 = 0,\ m_0(t) = 1$, and $m_n(0) = \int_{\mathbb{R}^d} |v|^{2n} f_0(v)dv$. These recursion formulas are also obtained using the weak formulation (2.4) with polynomial, in the square of the magnitude, test functions.

2.1 Boltzmann collisional models with heating sources

A collisional model associated to the space homogeneous Boltzmann transport equation (2.1) with Grad cutoff assumption (2.5), can be modified in order to accommodate for an energy or 'heat source' like term $\mathcal{G}(f(t,v))$, where $\mathcal{G}$ is a differential or integral operator. In these cases, it is possible to obtain stationary states with finite energy as for the case of inelastic interactions. In such a general framework, the corresponding initial value problem model is

$$\begin{aligned} \frac{\partial}{\partial t} f(v,t) &= \zeta(t)\, Q(f,f)(v,t) + \mathcal{G}(f(t,v))\,, \\ f(v,0) &= f_0(v)\,, \end{aligned} \tag{2.11}$$

where the collision operator $Q(f,f)(v,t)$ is as in (2.4-2.5) and $\mathcal{G}(f(t,v))$ models a 'heating source' due to different phenomena to be specified below. The term $\zeta(t)$ may represent a mean field approximation that allows for proper time rescaling. See [6] and [15] for several examples for these type of models and additional references.

Following the analytical work initiated in [15] and [14] on Non-Equilibrium Stationary States (NESS), we study several computational simulations of non-conservative models for either elastic or inelastic collisions associated to (2.11). In all cases we have addressed, the model have admissible stationary states with finite energy but they may not be Maxwellian distributions. Among several models with non-Maxwellian equilibrium state with finite energy, we study a computational output for three of the possible cases. The first one is a pure diffusion thermal bath due to a randomly heated background [59; 50; 34], where

$$\mathcal{G}_1(f) = \mu\, \Delta f, \tag{2.12}$$

where $\mu > 0$ is a constant. The second example relates to self-similar solutions of equation (2.11) for $\mathcal{G}(f) = 0$ [46; 25], but dynamically rescaled by

$$f(v,t) = \frac{1}{v_0^d(t)}\, \tilde{f}\Big(\tilde{v}(v,t), \tilde{t}(t)\Big), \quad \tilde{v} = \frac{v}{v_0(t)}, \tag{2.13}$$

where

$$v_0(t) = (a+\eta t)^{-1}, \quad \tilde{t}(t) = \frac{1}{\eta}\ln(1+\frac{\eta}{a}t), \quad a,\, \eta > 0. \tag{2.14}$$

Then, the equation for $\tilde{f}(\tilde{v},\tilde{t})$ coincides (after omitting the tildes) with equation (2.11), for

$$\mathcal{G}_2(f) = -\eta\, \mathrm{div}(vf), \qquad \eta > 0\,. \tag{2.15}$$

Of particular interest is the case for dynamically time-thermal speed self-similar rescaling corresponding to Maxwell type of interactions. Since the second moment of the collisional integral is a linear function of the energy, the energy evolves exponentially with a rate proportional to the energy production rate, that is

$$\frac{d}{dt}\mathcal{E}(t) = \lambda_0\, \mathcal{E}(t), \qquad \text{or equivalently } \mathcal{E}(t) = \mathcal{E}(0)\, e^{\lambda_0 t}\,, \tag{2.16}$$

with λ_0 being the energy production rate. Therefore the corresponding rescaled variables on equations (2.13) and (2.11),(2.15) for the study of long time behavior of rescaled solutions are

$$f(v,t) = \mathcal{E}^{-\frac{d}{2}}(t)\, \tilde{f}\Big(\frac{v}{\mathcal{E}^{\frac{1}{2}}(t)}\Big) = (\mathcal{E}(0)e^{\lambda_0 t})^{-\frac{d}{2}}\, \tilde{f}(v\,(\mathcal{E}(0)e^{\lambda_0 t})^{-\frac{1}{2}})\,, \tag{2.17}$$

and $\tilde{f}$ satisfies the self-similar equation (2.11) and

$$\mathcal{G}_{2'}(f) = -\lambda_0 x f_x, \tag{2.18}$$

where $x = v\mathcal{E}^{-\frac{1}{2}}(t)$ is the self-similar variable.

It has been shown that these dynamically scaled self-similar states are stable under very specific scaling for a large class of initial states [12], and we will use this analysis in order to adapt our scheme to compute the approximation to these self-similar states.

The last source type we consider is given by a model, related to a weakly coupled mixture modeling a slowdown or cooling process [14] for elastic Maxwell type of interactions of particles with mass $\mathbf{m}$ in the presence of a thermostat given by the Maxwellian distribution

$$M_{\mathcal{T}}(v) = \frac{\mathbf{m}}{(2\pi\mathcal{T})^{d/2}} e^{\frac{-\mathbf{m}|\mathbf{v}|^{\mathbf{2}}}{2\mathcal{T}}} \ ,$$

with a constant reference background or thermostat temperature $\mathcal{T}$ (i.e. the average of $\int M_{\mathcal{T}}\, dv = 1$ and $\int |v|^2 M_{\mathcal{T}}\, dv = \mathcal{T}$). We define

$$Q_L(f)(v,t) \doteq \int_{w\in\mathbb{R}^d, \sigma\in S^{d-1}} B_L(|u|,\mu) f(v',t) M_{\mathcal{T}}(w') - f(v,t) M_{\mathcal{T}}(w)]\, d\sigma dw\,. \tag{2.19}$$

Then, the corresponding initial value problem associated to $f(v,t)$ is given by

$$\begin{aligned} \frac{\partial}{\partial t} f(v,t) &= Q(f,f)(v,t) + \Theta Q_L(f)(v,t) \\ f(v,0) &= f_0(v)\,. \end{aligned} \tag{2.20}$$

where $Q(f,f)$ as defined in (2.4-2.5), is the classical collision integral for elastic interactions (i.e. $\beta = 1$) in weak form, so it conserves density, momentum and energy. The second integral term in (2.20) is a linear collision integral which conserves just the density (but not momentum or energy). The particle interaction law is given by

$$\begin{aligned} u &= v - w \qquad\qquad\qquad \text{the relative velocity} \\ v' &= v + \frac{\mathbf{m}}{\mathbf{m}+\mathbf{1}}(|u|\sigma - u), \qquad w' = w - \frac{1}{\mathbf{m}+\mathbf{1}}(|u|\sigma - u)\,. \end{aligned} \tag{2.21}$$

The coupling constant Θ depends on the initial density, the coupling constants and on $\mathbf{m}$. The collision kernel B_L of the linear part may not be the same as the one for the non-linear part of the collision integral, however we assume that the *Grad cut-off assumption* (2.6) is satisfied and that, in order to secure mass

preservation, the corresponding differential cross section functions b_N and b_L, the non-linear and linear collision kernels respectively, satisfy the renormalized condition

$$\int_{S^{d-1}} b_N(\frac{u\cdot\sigma}{|u|}) + \Theta b_L(\frac{u\cdot\sigma}{|u|})\, d\sigma \;=\; 1+\Theta\,. \tag{2.22}$$

This last model describes the evolution of binary interactions of two sets of particles, heavy and light, in a weakly coupled limit, where the heavy particles have reached equilibrium. The heavy particle set constitutes the background or thermostat for the lighter set of particles. It is the light particle distribution that is modeled by (2.20), so $Q(f,f)$ corresponds to all collisions that light particles have with each other, and the second linear integral term corresponds to collisions between light and heavy particles, where the heavy particles are at equilibrium with a distribution given by the classical Maxwellian $M_{\mathcal{T}}(v)$. Even though the local interactions are reversible (elastic), it does not conserve the total energy. In this binary 3-dimensional, mixture scenario, collisions are assumed to be isotropic, elastic and the interactions kernels of Maxwell type.

When considering the case of Maxwell type of interactions in three dimensions i.e. $B(|u|,\mu) = b(\theta)$ with a cooling background process corresponding to a time temperature transformation, $\mathcal{T} = \mathcal{T}(t)$ such that $\mathcal{T}(t) \to 0$ as $t \to 0$, the models have self-similar asymptotics [14; 12] for a large class of initial states. Such long time asymptotics corresponding to dynamically scaled solutions of (2.20), in the form of (2.18), yields interesting behavior in $f(v,t)$ for large time, converging to states with power like decay tails in v. In particular, such a solution $f(v,t)$ of (2.20) will lose moments as time grows, even if the initial state has all moments bounded. (see [14; 12] for the analytical proofs).

In the case of equal mass (i.e. $\mathbf{m} = \mathbf{1}$), the model is of particular interest for the development of numerical schemes and benchmarking of simulations. In such a case, there exists a special set of explicit self-similar solutions, in spectral space, which are attractors for a large class of initial states (see Section 4 for details).

2.2 Collision Integral Representation

One of the pivotal points in the derivation of the spectral numerical method for the computation of the non-linear Boltzmann equation lays in the representation of the collision integral in Fourier space by means of its weak form (2.4-2.5). In particular, taking $\psi(v) = e^{-i\zeta\cdot v}/(\sqrt{2\pi})^d$, where ζ is the Fourier variable, we get the Fourier transform of the collision integral as

$$\widehat{Q}(\zeta) = \frac{1}{(\sqrt{2\pi})^d} \int_{v\in\mathbb{R}^d} Q(f,f) e^{-i\zeta\cdot v} dv$$
$$= \int_{(w,v)\in\mathbb{R}^d\times\mathbb{R}^d,\, \sigma\in S^{d-1}} f(v)f(w) \frac{B(|u|,\mu)}{(\sqrt{2\pi})^d} [e^{-i\zeta\cdot v'} - e^{-i\zeta\cdot v}] d\sigma dw dv \,. \quad (2.23)$$

We use the notation $\widehat{\cdot} = \mathcal{F}(.)$ - the Fourier transform and $\mathcal{F}^{-1}$ for the classical inverse Fourier transform. Plugging in the definitions of collision kernel $B(|u|,\mu) = b_{\lambda,\beta}(\sigma)|u|^\lambda$ (which in the case of isotropic collisions would just be the variable hard sphere collision kernel) and of post-collisional velocity v'

$$\widehat{Q}(\zeta) = \frac{1}{(\sqrt{2\pi})^d} \int_{u\in\mathbb{R}^d} G_{\lambda,\beta}(u,\zeta) \int_{v\in\mathbb{R}^d} f(v)f(v-u) e^{-i\zeta\cdot v} dv du$$
$$= \int_{u\in\mathbb{R}^d} G_{\lambda,\beta}(u,\zeta) \mathcal{F}[f(v)f(v-u)] du \,, \quad (2.24)$$

where

$$G_{\lambda,\beta}(u,\zeta) = \int_{\sigma\in S^{d-1}} b_{\lambda,\beta}(\sigma)|u|^\lambda [e^{-i\frac{\beta}{2}\zeta\cdot(|u|\sigma - u))} - 1] d\sigma$$
$$= |u|^\lambda \left[e^{i\frac{\beta}{2}\zeta\cdot u} \int_{\sigma\in S^{d-1}} b_{\lambda,\beta}(\sigma) e^{-i\frac{\beta}{2}|u|\zeta\cdot\sigma} d\sigma - \omega_2 \right] . \quad (2.25)$$

Note that (2.25) is valid for both isotropic and anisotropic interactions. For the former type, a simplification ensues due to the fact the $b_{\lambda,\beta}(\sigma)$ is independent of $\sigma \in S^{d-1}$:

$$G_{\lambda,\beta}(u,\zeta) = b_{\lambda,\beta}\omega_{d-2}\,|u|^\lambda \left[e^{i\frac{\beta}{2}\zeta\cdot u} \mathrm{sinc}(\frac{\beta|u||\zeta|}{2}) - 1 \right] . \quad (2.26)$$

Thus, in the case of isotropic interaction the angular integration is given by the closed form above. In the case of anisotropic collisions, the dependence of $b_{\lambda,\beta}(\sigma)$ is calculated into a separate integral over the unit sphere S^{d-1} as given in (2.25). The above expression can be transformed for elastic collisions $\beta = 1$ into a form suggested by Rjasanow and Ibragimov in their paper [41]. The corresponding expression for anisotropic collisions is given by (2.25).

Further simplification of (2.24) is possible by observing that the Fourier transform inside the integral can be written in terms of the Fourier transform of $f(v)$ since it can also be written as a convolution of the Fourier transforms. Let $f_u(v) = f(v-u)$

$$
\begin{aligned}
\widehat{Q}(\zeta) &= \int_{u\in\mathbb{R}^d} G_{\lambda,\beta}(u,\zeta)\mathcal{F}(f\, f_u)(\zeta)du \\
&= \int_{u\in\mathbb{R}^d} G_{\lambda,\beta}(u,\zeta)\frac{1}{(\sqrt{2\pi})^d}(\hat{f} * \widehat{f_u})(\zeta)du \\
&= \int_{u\in\mathbb{R}^d} G_{\lambda,\beta}(u,\zeta)\frac{1}{(\sqrt{2\pi})^d}\int_{\xi\in\mathbb{R}^d}\hat{f}(\zeta-\xi)\widehat{f_u}(\xi)d\xi du \\
&= \int_{u\in\mathbb{R}^d} G_{\lambda,\beta}(u,\zeta)\frac{1}{(\sqrt{2\pi})^d}\int_{\xi\in\mathbb{R}^d}\hat{f}(\zeta-\xi)\hat{f}(\xi)e^{-i\xi\cdot u}d\xi du \\
&= \frac{1}{(\sqrt{2\pi})^d}\int_{\xi\in\mathbb{R}^d}\hat{f}(\zeta-\xi)\hat{f}(\xi)\hat{G}_{\lambda,\beta}(\xi,\zeta)d\xi, \qquad (2.27)
\end{aligned}
$$

where $\hat{G}_{\lambda,\beta}(\xi,\zeta) = \int_{u\in\mathbb{R}^d} G_{\lambda,\beta}(u,\zeta)e^{-i\xi\cdot u}du$. In particular, $\widehat{Q}(\zeta)$ is a weighted convolution in Fourier space.

Let $u = r\mathbf{e}$, $\mathbf{e}\in S^{d-1}, r\in\mathbb{R}$. For $d=3$, it follows

$$
\begin{aligned}
\hat{G}_{\lambda,\beta}(\xi,\zeta) &= \int_r\int_{\mathbf{e}} r^2 G(r\mathbf{e},\zeta)e^{-ir\xi\cdot\mathbf{e}}d\mathbf{e}dr \qquad (2.28)\\
&= 16\pi^2 C_\lambda\int_r r^{\lambda+2}[\mathrm{sinc}(\frac{r\beta|\zeta|}{2})\mathrm{sinc}(r|\xi-\frac{\beta}{2}\zeta|) - \mathrm{sinc}(r|\xi|)]dr\,.
\end{aligned}
$$

Since the domain of computation is restricted to $\Omega_v = [-L,L)^3$, $u\in[-2L,2L)^3$ then $r\in[0,2\sqrt{3}L]$, and the right hand side of (2.28) is the finite integral

$$
16\pi^2 C_\lambda\int_0^{2\sqrt{3}L} r^{\lambda+2}[\mathrm{sinc}(\frac{r\beta|\zeta|}{2})\mathrm{sinc}(r|\xi-\frac{\beta}{2}\zeta|) - \mathrm{sinc}(r|\xi|)]dr\,. \qquad (2.29)
$$

A point worth noting here is that the above formulation (2.27) results in $O(N^{2d})$ number of operations, where N is the number of discretizations in each velocity direction. Also, exploiting the symmetric nature in particular cases of the collision kernel one can reduce the number of operations to $O(N^d logN)$ in velocity space (or $NlogN$ if N counts the total number of Fourier nodes in d dimensional velocity space).

3 Numerical Method

3.1 Discretization of the Collision Integral

Coming to the discretization of the velocity space, it is assumed that the two interacting velocities and the corresponding relative velocity

$$
v\,, w\,,\ u\ \in[-L,L)^d \qquad \text{and} \qquad \zeta\ \in[-L_\zeta,L_\zeta)^d\,, \qquad (3.1)
$$

where the velocity domain L is chosen such that $u = v - w \in [-L, L)^d$ through an assumption that $supp(f) \in [-L, L)^d$. For a sufficiently large L, the computed distribution will not lose mass, since the initial momentum is conserved (there is no convection in space homogeneous problems), and is renormalized to zero mean velocity. We assume a uniform grid in the velocity and Fourier spaces with h_v and h_ζ as the respective grid element sizes. h_v and h_ζ are chosen such that $h_v h_\zeta = \frac{2\pi}{N}$, where N = number of discretizations of v and ζ in each direction as a requirement for using a standard FFT package.

3.2 Time Discretization

In the process of getting a dimensionless formulation, we recall the basic rescaling for the Boltzmann equation. First we defined the *mean free path* as the product of the average speed by the *mean free time* (the average time between collisions which depends on the collision frequency). The *mean free path* is the average distance traveled between collisions, and it is very relevant for space dependent solutions.
In the case of space homogeneous simulations, we use a second-order Runge-Kutta scheme or a Euler forward step method for approximation to the time derivative of f, where the value of dimensionless time step dt is chosen of the order 0.1 times *mean free time*
With time discretizations taken as $t^n = ndt$, the discrete version of the Runge-Kutta scheme we use is given by

$$\begin{aligned} f^0(v^j) &= f_0(v^j) \\ \tilde{f}(v^j) &= f^{t^n}(v^j) + \frac{dt}{2} Q_{\lambda,\beta}[f^{t^n}(v^j), f^{t^n}(v^j)] \\ f^{t^{n+1}}(v^j) &= f^{t^n}(v^j) + dt Q_{\lambda,\beta}[\tilde{f}(v^j), \tilde{f}(v^j)] \ , \end{aligned} \tag{3.2}$$

and the corresponding Forward Euler scheme with smaller time step is given by

$$\tilde{f}(v^j) = f^{t^n}(v^j) + dt Q(f^{t^n}, f^{t^n}) \qquad . \tag{3.3}$$

3.3 Conservation Properties - Lagrange Multipliers

Since the calculation of $Q_{\lambda,\beta}(f, f)(v)$ involves computing Fourier transforms with respect to v, we extensively use a Fast Fourier Transform method. Note that the total number of operations in computing the collision integral reduces to the order of $3N^{2d}log(N)+O(N^{2d})$ for (2.24) and $O(N^{2d})$ for (2.27). Observe that, choosing $1/2 \leq \beta \leq 1$, the proposed scheme works for both elastic and

inelastic collisions. As a note, the method proposed in the current work can also be extended to lower dimensions in velocity space.

The accuracy of the proposed method relies heavily on the size of the grid and the number of points taken in each velocity/Fourier space directions, where it be seen that the computed $Q_{\lambda,\beta}[f,f](v)$ does not conserve the quantities it is supposed to, when tested with the collision invariants. That is ρ, m, e must be conserved in time for elastic collisions, but just ρ for linear Boltzmann integral, and ρ, m for inelastic collisions. Even though the difference between the computed (discretized) collision integral and the continuous one may not be large, it is nevertheless essential that this issue be addressed and solved.

To this end, we propose a simple constrained Lagrange multiplier method is employed where the constraints are the required conservation properties on the moments for the solution.
Let $M = N^d$, the total number of discretizations of the velocity space. Assume that the classical Boltzmann collision operator is being computed. So $\rho, m = (m1, m2, m3)$ and e are conserved. Let ω_j be the integration weights where $j = 1, 2, ..., M$. Let

$$\tilde{f} = \begin{pmatrix} \tilde{f}_1 & \tilde{f}_2 & . & . & \tilde{f}_M \end{pmatrix}^T$$

be the distribution vector at the computed time step and

$$f = \begin{pmatrix} f_1 & f_2 & . & . f_M \end{pmatrix}^T$$

be the constructed corrected distribution vector with the required moments conserved. Let

$$C_{(d+2)\times M} = \begin{pmatrix} \omega_j \\ v_i\omega_j \\ |v_j|^2\omega_j \end{pmatrix}$$

and

$$a_{(d+2)\times 1} = \begin{pmatrix} \rho & m1 & m2 & m3 & e \end{pmatrix}^T$$

be the vector of conserved quantities. The corresponding conservation scheme can be written as the following constrained optimization problem:

$$\begin{aligned} &\text{Given } \tilde{f} \in \mathbb{R}^M, C \in \mathbb{R}^{d+2\times M}, \text{ and } a \in \mathbb{R}^{d+2}, \\ &\qquad \text{find } f \in \mathbb{R}^M \text{ such that} \\ &\text{minimizes } \|\tilde{f} - f\|_2^2, \text{ subject to the constrain } Cf = a. \end{aligned} \tag{3.4}$$

To solve this constrain minimization problem, we employ the Lagrange mul-

tiplier method. Let $\lambda \in \mathbb{R}^{d+2}$ be the Lagrange multiplier vector. Then the corresponding scalar objective function to be optimized is given by

$$L(f, \lambda) = \sum_{j=1}^{M} |\tilde{f}_j - f_j|^2 + \lambda^T (Cf - a)\,. \tag{3.5}$$

Equation (3.5) can actually be solved explicitly for the corrected distribution value and the resulting equation of correction can be implemented numerically in the code. Taking the derivative of $L(f, \lambda)$ with respect to $f_j, j = 1, ..., M$ and $\lambda_i, i = 1, ..., d+2$ i.e. gradients of L,

$$\frac{\partial L}{\partial f_j} = 0;\ j = 1, ..., M \qquad \Rightarrow \quad f = \tilde{f} + \frac{1}{2} C^T \lambda\,,$$

and

$$\frac{\partial L}{\partial \lambda_1} = 0;\ i = 1, ..., d+2 \quad \Rightarrow \quad Cf = a\,, \tag{3.6}$$

retrieves the constraints. Solving for λ,

$$CC^T \lambda = 2(a - C\tilde{f})\,. \tag{3.7}$$

Recall that CC^T is symmetric and positive definite, since C is the integration matrix, then the inverse of CC^T exists. In particular the value of λ is determined by

$$\lambda = 2(CC^T)^{-1}(a - C\tilde{f})\,. \tag{3.8}$$

Then, substituting λ into (3.6) we obtain,

$$f = \tilde{f} + C^T (CC^T)^{-1}(a - C\tilde{f})\,, \tag{3.9}$$

and using equation for forward Euler scheme (3.3), the complete scheme is given by

$$\begin{aligned} \tilde{f}_j &= f_j^n + dtQ(f_j^n, f_j^n) \\ f_j^{n+1} &= \tilde{f}_j + C^T (CC^T)^{-1}(a - C\tilde{f}) \ \ \forall j\,, \qquad \text{with} \ \ f^{t^n}(v^j) = f_j^n \ . \end{aligned} \tag{3.10}$$

Then ,

$$\begin{aligned} f_j^{n+1} &= f_j^n + dtQ(f_j^n, f_j^n) + C^T (CC^T)^{-1}(a - C\tilde{f}) \\ &= f_j^n + dtQ(f_j^n, f_j^n) + C^T (CC^T)^{-1}(a - a - dtCQ(f_j^n, f_j^n)) \\ &= f_j^n + dtQ(f_j^n, f_j^n) - dtC^T (CC^T)^{-1} CQ(f_j^n, f_j^n) \\ &= f_j^n + dt[\mathbb{I} - C^T (CC^T)^{-1} C]Q(f_j^n, f_j^n)\,, \end{aligned} \tag{3.11}$$

with $\mathbb{I}$ - $N \times N$ identity matrix. Letting $\Lambda_N(C) = \mathbb{I} - C^T(CC^T)^{-1}C$ with $\mathbb{I}$ - $N \times N$ identity matrix, one obtains

$$f_j^{n+1} = f_j^n + dt\Lambda_N(C)Q(f_j^n, f_j^n)\,, \tag{3.12}$$

where we expect the required observables are conserved and the solution approaches a stationary state, since $\lim_{n\to\infty} \|\Lambda_N(C)\, Q(f_j^n, f_j^n)\|_\infty = 0$.

Identity (3.12) summarizes the whole conservation process. Moreover, the optimization method can be extended to have the distribution function satisfy higher order moments from (2.10). In this case, $a(t)$ will include entries of $m_n(t)$ from (**??**).

We point out that for the linear Boltzmann collision operator used in the mixture problem conserves density and not momentum (unless one computes isotropic solutions) and energy. For this problem, the constraint would just be the density equation. For inelastic collisions, density and momentum are conserved and in this case the constraints are the energy and momentum equations. For the elastic Boltzmann operator, all three quantities (density, momentum and energy) are conserved and this approximated quantities are the constraints for the optimization problem. This approach of using Lagrangian constraints in order to secure moment preservation differs from the proposed in [27], [28] for conservation of moments using spectral solvers.

4 Self-Similar asymptotics for a general elastic or inelastic BTE of Maxwell type or the cold thermostat problem - power law tails

As mentioned in the introduction, a new interesting benchmark problem for our scheme is the capability to compute dynamically scaled solutions or self-similar asymptotics. More precisely, we present simulation where the computed solution, in a properly scaled time, approaches an admissible self-similar solution. Such procedure yields a choice of non-equispaced time grid depending on the spectral properties of the model being computed. And, in fact, such a choice in the time rescaling for self-similarity asymptotic approximations in Fourier space are actually a choice of a non-equispaced grid in Fourier space since the self-similarity variable is a proportion of the quotient of velocity and time as shown in (2.16, 2.17, 2.18 for Maxwell type models. Equivalently, in the corresponding Fourier transformed framework, it is a proportion of the quotient of the spectral (Fourier) variable and time. This is actually the same qualitative issue that is needed for the calculation of the heat equation kernel (or fundamental solution) by means of non-equispaced grids in Fourier space in [39]. We recall that the fundamental solution for the initial value problem associated to the heat equation is actually the self-similar solution the heat

equation.

This procedure is of particular interest for our method because of the power tail behavior of the asymptotic self-similar state, i.e. higher order moments of the computed solution will become unbounded in properly rescaled time. The computational method and proposed scheme is be benchmarked with an available explicit solution for a particular choice of parameters. For the completeness of this presentation, the analytical description of such asymptotics is given in the following two sub sections.

4.1 Self-Similar Solution for a non-negative Thermostat Temperature

We consider the Maxwell type equation from (2.20) related to a space homogeneous model for a weakly coupled mixture modeling slowdown process. The content of this section is dealt in detail in [14] for a particular choice of zero background temperature (cold thermostat). For the sake of brevity, we refer to [14] for details. However, a slightly more general form of the self-similar solution for non zero background temperature is derived here from the zero background temperature solution. Without loss of generality for our numerical test, we assume the differential cross sections b_L for collision kernel of the linear and b_N, the corresponding one for the nonlinear part, are the same, both denoted by $b(\frac{k.\sigma}{|k|})$, satisfying the *Grad cut-off* conditions (2.6). In particular, condition (2.22) is automatically satisfied.

In [14], it was shown that the Fourier transform of the isotropic self-similar solution associated to problem in (2.20) takes the form:

$$\phi(x,t) \;=\; \psi(xe^{-\mu t}) \;=\; 1-a(xe^{-\mu t})^p, \quad \text{as} \quad xe^{-\mu t}\to 0, \quad \text{with} \quad p\le 1\,, \tag{4.1}$$

where $x=|\zeta|^2/2$ and μ and Θ are related by

$$\mu \;=\; \frac{2}{3p^2} \quad \text{and} \quad \Theta \;=\; \frac{(3p+1)(2-p)}{3p^2}\,.$$

Note that $p=1$ corresponds to initial states with finite energy. It was shown in [14] for $\mathcal{T}=0$ (i.e. a cold thermostat effect), the Fourier transform of the self-similar, isotropic solutions of (2.20) is given by

$$\phi(x,t)=\frac{4}{\pi}\int_0^\infty \frac{1}{(1+s^2)^2}e^{-xe^{\frac{-2t}{3}}as^2}ds\,, \tag{4.2}$$

and its corresponding inverse Fourier transform, both for $p = 1$, $\mu = \frac{2}{3}$ and $\Theta = \frac{4}{3}$ (as computed in [14]) is given by

$$f_0^{ss}(|v|,t) = e^t F_0(|v|e^{t/3}) \quad \text{with} \quad F_0(|v|) = \frac{4}{\pi}\int_0^\infty \frac{1}{(1+s^2)^2}\frac{e^{-|v|^2/2s^2}}{(2\pi s^2)^{\frac{3}{2}}}ds. \tag{4.3}$$

Remark: *It is interesting to observe that, as computed originally in [9], for $p = \frac{1}{3}$ or $p = \frac{1}{2}$ in (4.2) yields $\Theta = 0$, which corresponds to the classical elastic model of Maxwell type. In this case it is possible to construct explicit solutions to the elastic BTE with infinite initial energy. In addition, it is clear now that in order to have self-similar explicit solutions with finite energy in the case of the classical elastic model of Maxwell type one needs to have an extra "source term" such as a weakly couple mixture model for slowdown processes, or bluntly speaking the linear collisional term added to the elastic energy conservative operator.*

In order to recover the self-similar solution for the original equilibrium positive temperature $\mathcal{T}$ (i.e. hot thermostat case) for the linear collisional term, we denote, including time dependence for convenience,

$$\begin{aligned} \phi_0(x,t) \;=\; \phi(x,t)_{Thermostat=0} \quad \text{and} \quad \phi_{\mathcal{T}}(x,t) \;=\; \phi(x,t)_{Thermostat=\mathcal{T}} \\ \text{so that} \quad \phi_{\mathcal{T}}(x,t) \;=\; \phi_0(x,t)e^{-\mathcal{T}x}\,. \end{aligned} \tag{4.4}$$

Note that the solution constructed in (4.2) is actually $\phi_0(x,t)$. Then the self-similar solution for non zero background temperature, denoted by $\phi_{\mathcal{T}}(x,t)$ satisfies

$$\begin{aligned} \phi_{\mathcal{T}}(k,t) &= \frac{4}{\pi}\int_0^\infty e^{-|k|^2 e^{-2t/3}as^2/2}\frac{1}{(1+s^2)^2}e^{-|k|^2\mathcal{T}/2}ds \\ &= \frac{4}{\pi}\int_0^\infty e^{-|k|^2[e^{-2t/3}as^2+\mathcal{T}]/2}\frac{1}{(1+s^2)^2}ds. \end{aligned} \tag{4.5}$$

In particular, letting $\bar{T} = e^{-2t/3}as^2 + \mathcal{T}$ and taking the inverse Fourier Transform, we obtain the corresponding self-similar state for the positive temperature thermostat, which according to (2.17) the can be written in probability space as follows

$$f_{\mathcal{T}}^{ss}(|v|,t) = e^t F_{\mathcal{T}}(|v|e^{t/3})\,, \qquad F_{\mathcal{T}}(|v|) = \frac{4}{\pi}\int_0^\infty \frac{1}{(1+s^2)^2}\frac{e^{-|v|^2/2\bar{T}}}{(2\pi\bar{T})^{\frac{3}{2}}}ds. \tag{4.6}$$

Then, letting $t \to \infty$, since $\bar{T} = \mathcal{T} + as^2 e^{\frac{-2t}{3}} \to \mathcal{T}$, yields

$$F_{\mathcal{T}}(|v|) \to_{t\to\infty} \frac{4}{\pi}\frac{1}{(2\pi\mathcal{T})^{\frac{3}{2}}} e^{-|v|^2/2\mathcal{T}} \int_0^\infty \frac{1}{(1+s^2)^2} ds = M_{\mathcal{T}}(v)\,, \tag{4.7}$$

$$\text{since} \qquad \frac{4}{\pi}\int_0^\infty \frac{1}{(1+s^2)^2} ds \;=\; \frac{2}{\pi}\left(\frac{s}{1+s^2} + \arctan(s)\right)|_0^\infty = \; 1. \tag{4.8}$$

Then, the self-similar particle distribution $f^{ss}_{\mathcal{T}}(v,t)$ for the positive temperature thermostat approaches a rescaled Maxwellian distribution with the background temperature $\mathcal{T}$, that is, according to (2.17)

$$f^{ss}_{\mathcal{T}}(|v|,t) \;=\; e^t F_{\mathcal{T}}(|v|e^{t/3}) \approx \frac{e^t}{(2\pi\mathcal{T})^{\frac{3}{2}}}\, e^{-(|v|^2\, e^{2t/3})/2\mathcal{T}+t}\,, \quad \text{as } t\to\infty\,. \tag{4.9}$$

Remark: *As pointed out in the previous remark, such asymptotic behavior, for finite initial energy, is due to the balance of the binary term and the linear collisional term in* (2.20).
In addition, very interesting behavior is seen on $F_{\mathcal{T}}(|v|)$ as $\mathcal{T}\to 0$ (cold thermostat problem), where the particle distribution approaches a distribution with power-like tails (i.e. a power law decay for large values of $|v|$) and an integral singularity at the origin. Indeed, is derived in [14] the asymptotic behavior of $F_0(|v|)$ from (4.3), for large and small values of $|v|$, leading to

$$\begin{aligned} F_0(|v|) &= 2(\frac{2}{\pi})^{5/2}\frac{1}{|v|^6}[1+O(\frac{1}{|v|})], \quad \text{for } \; |v|\to\infty, \\ F_0(|v|) &= \frac{2^{1/2}}{\pi^{5/2}}\frac{1}{|v|^2}[1+2|v|^2 ln(|v|)+O(|v|^2)], \quad \text{for } \; |v|\to 0. \end{aligned} \tag{4.10}$$

In particular, the self-similar particle distribution function $F_0(|v|)$, $v\in\mathbb{R}^3$, behaves like $\frac{1}{|v|^6}$ as $|v|\to\infty$, and as $\frac{1}{|v|^2}$ as $|v|\to 0$, which indicates a very anomalous, non-equilibrium behavior as function of velocity, which nevertheless remains with finite mass and kinetic energy. This asymptotic effect can be described as an overpopulated (with respect to Maxwellian), large energy tails and infinitely many particles at zero energy. This interesting, unusual behavior is observed in problems of soft condensed matter [38].

We shall see in the following section that our solver captures these states described above with spectral accuracy since the self-similar solutions are attractors for a large class of initial states. These numerical tests are a crucial aspect of the spectral Lagrangian deterministic solver used to simulate this type of non-equilibrium phenomena, where all these explicit formulae for our probability distributions allow us to carefully benchmark the proposed numerical scheme. First we recall some relevant analytical results that secure the convergence to these particular self-similar states.

The self-similar nature of the solutions $F(|v|)$ for a very general class of problems of Maxwell type interactions, for a wide range of values for the parameters β, p, μ and Θ, was addressed in [12] in much detail. Three different behaviors have been clearly explained. Of particular interest for our present numerical study are the mixture problem with a cold background and the inelastic Boltzmann cases. Interested readers are referred to [12].

For the purpose of our presentation, let $\phi = \mathcal{F}[f]$ be the Fourier transform of the probability distribution function satisfying the initial value problem (2.1)-(2.5) or (2.11) and let $\Gamma(\phi) = \mathcal{F}[Q^+(f,f)]$ be the Fourier transform of the gain part of the collisional term associated with the initial value problem for $f(v,0) = f_0(v)$ prescribed. It was shown in [12] that the operator $\Gamma(\phi)$, defined over the Banach space of continuous bounded functions with the L^∞-norm (i.e. the space of characteristic functions, that is the space of Fourier transforms of probability distributions), satisfies the following three properties [12]:

1 - $\Gamma(\phi)$ preserves the unit ball in the Banach space.

2 - $\Gamma(\phi)$ is L-Lipschitz operator, i.e. there exists a bounded linear operator L in the Banach space, such that

$$|\Gamma(\phi_1) - \Gamma(\phi_2)|(x,t) \;\le\; L(|\phi_1 - \phi_2|(x,t)), \quad \forall\ \|\phi_i\| \le 1; i = 1,2\,. \tag{4.11}$$

3 - $\Gamma(\phi)$ is invariant under transformations (dilations)

$$e^{\tau\mathcal{D}}\Gamma(\phi) = \Gamma(e^{\tau\mathcal{D}}\phi)\ , \quad \mathcal{D} = x\frac{\partial}{\partial x}\ , \quad e^{\tau\mathcal{D}}\phi(x) = \phi(xe^{\tau}), \quad \tau \in \mathbb{R}^+\ . \tag{4.12}$$

In the particular case of the initial value problem associated to Boltzmann type of equations for Maxwell type of interactions, the bounded linear operator that satisfies property **2** is the one that linearizes the Fourier transform of the gain operator about the state $\phi = 1$.

Next, let x^p, restricted to the unit ball, be the eigenfunction corresponding to the eigenvalue $\lambda(p)$ of the linear operator L associated to Γ in (4.11), i.e. $L(x^p) = \lambda(p)x^p$. Also let

$$\mu(p) = \frac{\lambda(p) - 1}{p} \quad \text{be defined for} \quad p > 0\,, \tag{4.13}$$

and called the *spectral function associated to* Γ. It was shown in [12] that $\mu(0+) = +\infty$ (i.e. $p = 0$ is a vertical asymptote) and that for the problems associated to the initial value problems (2.1)-(2.5) or (2.11), there exists a unique minimum for $\mu(p)$ localized at $p_0 > 1$, and that $\mu(p) \to 0^-$ as $p \to +\infty$.

Then, the existence of self-similar states and convergence of the solution to the initial value problem to such a self-similar distribution function was described and proved in [12], and it is summarized in the following four statements:

(i) Lemma (existence and uniqueness of the initial value problem): There exists a unique isotropic solution $f(|v|,t)$ to the initial value problem (2.1)-(2.5) or (2.11) for Maxwell type interactions, in the class of probability measures, satisfying $f(|v|,0) = f_0(|v|) \geq 0, \int_{\mathbb{R}^d} f_0(|v|)dv = 1$ such that for the Fourier transform problem $x = \frac{|\zeta|^2}{2}, u_0 = \mathcal{F}[f_0(|v|)] = 1 + O(x)$, as $x \to 0$,

(ii) Theorem (existence of self-similar states): $f(|v|,t)$ has self-similar state in the following sense: Assume that the Fourier transform of the initial state satisfies

$$u_0 + \mu(p)\ x^p\ u_0' = \Gamma(u_0) + O(x^{p+\epsilon}), \quad \text{such that} \quad p + \epsilon < p_0\,, \tag{4.14}$$

(i.e. $\mu(p); \mu'(p) < 0$), where $\mu(p)$ is the spectral function defined in (4.13). Then, there exists a unique, non-negative, self-similar solution

$$f^{ss}(|v|,t) = e^{-\frac{d}{2}\mu(p)t} F_p(|v|e^{-\frac{1}{2}\mu(p)t})\,,$$

with $\mathcal{F}(F_p(|v|)) = w(x), x = |\zeta|^2/2$ such that $\mu(p)x^p w'(x) + w(x) = \Gamma(w)$.

(iii) Theorem (self-similar asymptotics): There exists a unique (in the class of probability measures) solution $f(|v|,t)$ satisfying $f(|v|,0) = f_0(|v|) \geq 0$, with $\int_{\mathbb{R}^d} f(|v|)dv = 1$, such that for $x = \frac{|\zeta|^2}{2} \to 0$ and

$$\mathcal{F}[f_0(|v|)] = 1 - a\,x^p + O(x^{p+\epsilon}), 0 \leq p \leq 1 \quad \text{with } p + \epsilon < p_0\ .$$

Then, there exists a unique non-negative self-similar solution $f_{ss}^{(p)}(|v|,t) = e^{-\frac{d}{2}\mu(p)t} F_p(|v|e^{-\frac{1}{2}\mu(p)t})$ for any given $0 \leq p \leq 1$, such that

$$f(|v|,t) \to_{t\to\infty} e^{-\frac{d}{2}\mu(p)t} F_p(|v|e^{-\frac{1}{2}\mu(p)t})\ . \tag{4.15}$$

or equivalently

$$e^{\frac{d}{2}\mu(p)t} f(|v|e^{\frac{1}{2}\mu(p)t}, t) \to_{t\to\infty} F_p(|v|)\ , \tag{4.16}$$

where $\mu(p)$ is the value of spectral function (4.13) associated to the linear bounded operator L .

(iv) Power tail behavior of the asymptotic limit: If $\mu(p) < 0$, then the self-similar limiting function $F_p(|v|)$ does not have finite moments of all orders. In addition, if $0 \leq p \leq 1$ then all moments of order less than p are bounded; i.e. $m_q = \int_{\mathbb{R}^d} F_p(|v|)|v|^{2q}dv \leq \infty; 0 \leq q \leq p$. However, if $p = 1$ (finite energy case) then, the boundedness of moments of any order larger than 1, depends on the conjugate value of $\mu(1)$, the spectral function $\mu(p)$. That means $m_q \leq \infty$ only for $0 \leq q \leq p_*$, where $p_* \geq p_0 > 1$ is the unique maximal root of the equation $\mu(p_*) = \mu(1)$.

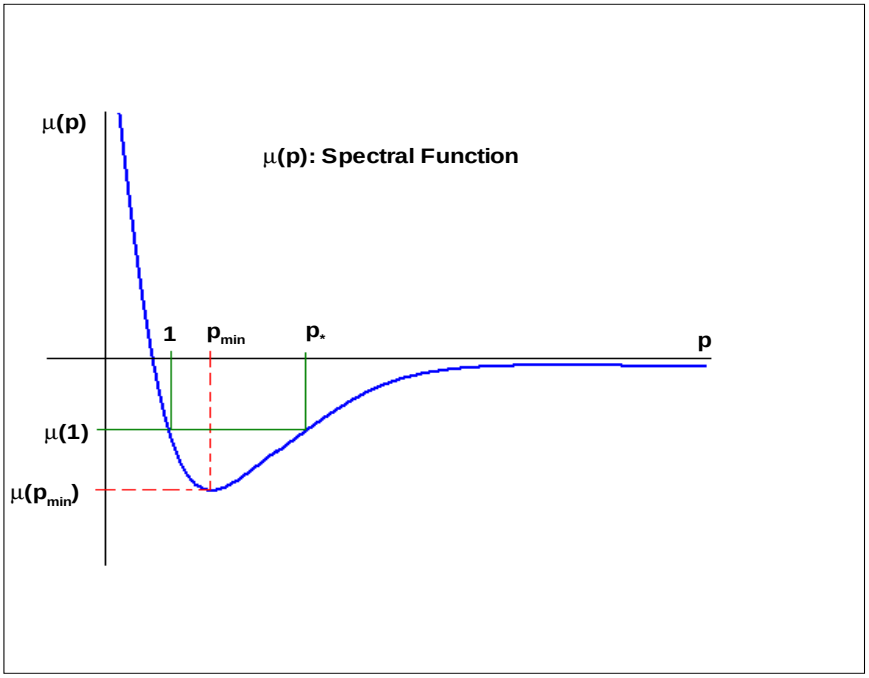

Fig. 1. Typical graph for the spectral function $\mu(p)$ for a general homogeneous Boltzmann collisional problem of Maxwell type

Remark 1: *When $p = 1$, $\mu(1)$ is the energy dissipation rate, and $\mathcal{E}(t) = e^{\mu(1)t}$ the kinetic energy evolution function. So, $\mathcal{E}(t)^{d/2} f(v\mathcal{E}(t), t) \to F_1(|v|)$.*

Remark 2: *We point out that condition* (4.14) *on the initial state is easily satisfied by taking a sufficiently concentrated Maxwellian distribution as shown in [12], and as done for our simulations in the next section.*

However, when rescaling with a different rate in time, it is not possible to pick up the non-trivial limiting state f^{ss}, since, as shown in [12],

$$f(|v|e^{\frac{1}{2}\eta t}, t) \to_{t\to\infty} e^{-\frac{d}{2}\eta t}\delta_0(|v|); \quad \eta > \mu(1)\,, \tag{4.17}$$

and

$$f(|v|e^{\frac{1}{2}\eta t}, t) \to_{t\to\infty} 0; \quad \mu(p_{min}) < \mu(1+\delta) < \eta < \mu(1)\,. \tag{4.18}$$

These results are also true for any $p \leq 1$. For the general space homogeneous (elastic or inelastic) Boltzmann model of Maxwell type or the corresponding mixture problem, the spectral function $\mu(p)$, as defined in (4.13), is given in figure 1.

5 Numerical Results

We benchmark the proposed numerical method to compute several examples in three dimensions, both in velocity and time, for several initial value problems associated with non-conservative models where some analysis is available, as are exact moment formulae for Maxwell type of interactions as well as qualitative analysis for solutions of VHS models. We shall plot our numerical results versus the exact available solutions when available. Because all computed problems converge to an isotropic long time state, we choose to plot the distribution function in only one direction, which is chosen to be the one with the initial anisotropies in velocity space. All the numerical simulations considered in this manuscript correspond to examples with space homogeneous, isotropic, VHS collision kernels, i.e. differential cross section independent from scattering angle.

We simulate the homogeneous problem associated to the following problems for different choices of the parameters β and λ, and the Jacobian J_β and heating force term $\mathcal{G}(f)$.

5.1 Maxwell type of Elastic Collisions

Consider the initial value problem (2.1), (2.2), with $B(|u|,\mu) = \frac{1}{4\pi}|u|^\lambda$ with the value of the parameters are $e = \beta = 1,\ J_\beta = 1,\ \lambda = 0$ and with the pre-collisional velocities defined from (2.3). In this case, for a general initial state with finite mass, mean and kinetic energy, there is no exact expression for the evolving distribution function. However there are exact expressions for all the statistical moments (observables). Thus, the numerical method is compared with the known analytical moments for different discretizations in the velocity space.

The initial states we take are convex combinations of two shifted Maxwellian distributions. So consider the following case of initial states with unit mass $\int_{\mathbb{R}^3} f_0(v)dv = 1$ given by convex combinations of shifted Maxwellians

$$f(v,0) = f_0(t) = \gamma M_{T_1}(v - V_1) + (1-\gamma)M_{T_2}(v - V_2);\ \text{with } 0 \leqslant \gamma \leqslant 1$$

where $M_T(v - V) = \frac{1}{(2\pi T)^{3/2}} e^{\frac{-|v-V|^2}{(2T)}}$. Then, taking $\gamma = 0.5$ and mean fields for the initial state determined by

$$V_1 = [-2,2,0]^T\,, \qquad V_2 \ = \ [2,0,0]^T; \qquad T_1 = 1\,,\ \ T_2 \ = \ 1\,,$$

enables the first five moment equations corresponding to the collision invariants to be computed from those of the initial state. All higher order moments are computed using the classical moments recursion formulas for Maxwell type of interactions (2.10). In particular, it is possible to obtain the exact evolution of all moments as functions of time. Thus,

$$\rho(t) = \rho_0 = 1 \quad \text{and} \quad V(t) = V_0 = [0, 1, 0]^T \ ,$$

and, from the moments calculation in (2.10), the complete evolution of the second moment tensor (2.9) is given by

$$M(t) = \begin{pmatrix} 5 & -2 & 0 \\ -2 & 3 & 0 \\ 0 & 0 & 1 \end{pmatrix} e^{-t/2} + \frac{1}{3} \begin{pmatrix} 8 & 0 & 0 \\ 0 & 11 & 0 \\ 0 & 0 & 8 \end{pmatrix} (1 - e^{-t/2}) \, ,$$

the energy flow (2.9) by

$$r(t) = \frac{1}{2} \begin{pmatrix} -4 \\ 13 \\ 0 \end{pmatrix} e^{-t/3} + \frac{1}{6} \begin{pmatrix} 0 \\ 43 \\ 0 \end{pmatrix} (1 - e^{-t/3}) - \frac{1}{6} \begin{pmatrix} 12 \\ 4 \\ 0 \end{pmatrix} (e^{-t/2} - e^{-t/3}) \ ,$$

and the kinetic temperature is conserved, so

$$T(t) = T_0 = \frac{8}{3} \, ;$$

since the kinetic energy is also conserved, that is $\mathcal{E}(t) = \mathcal{E}(0)$ for all t.
These moments, along with their numerical approximations for different discretizations in velocity space, are plotted in figure 2. We took $N = 16$ for the numerical simulations and it can be seen that the computed moments agree almost exactly with the analytical results except for energy flow $r(t)$, a third order moment. This indicates that as higher order moments, such as $r(t)$ from (2.9), generate larger errors, and may diverge from the analytical solution for large times as it can be observed in the last two plots of the energy flow $r_1(t)$ and $r_2(t)$ in figure 2. This can be improved by increasing the value of N, the number of Fourier modes. We point out that it is also possible, in this case of Maxwell type interactions, to augment the number of constrains (i.e. the vector a) to include the time evolution of more explicit moment formulas, however this approach would only be useful for higher order computational accuracy of the Boltzmann equation of Maxwell type. Thus, for this presentation, we just constrain the lowest moments for which conservation holds independent of the collision rate. In figure 3, the evolution of the computed distribution function into a Maxwellian is plotted for $N = 40$, and it is still possible to see the error in both the components r_1, r_2 of the energy flow.

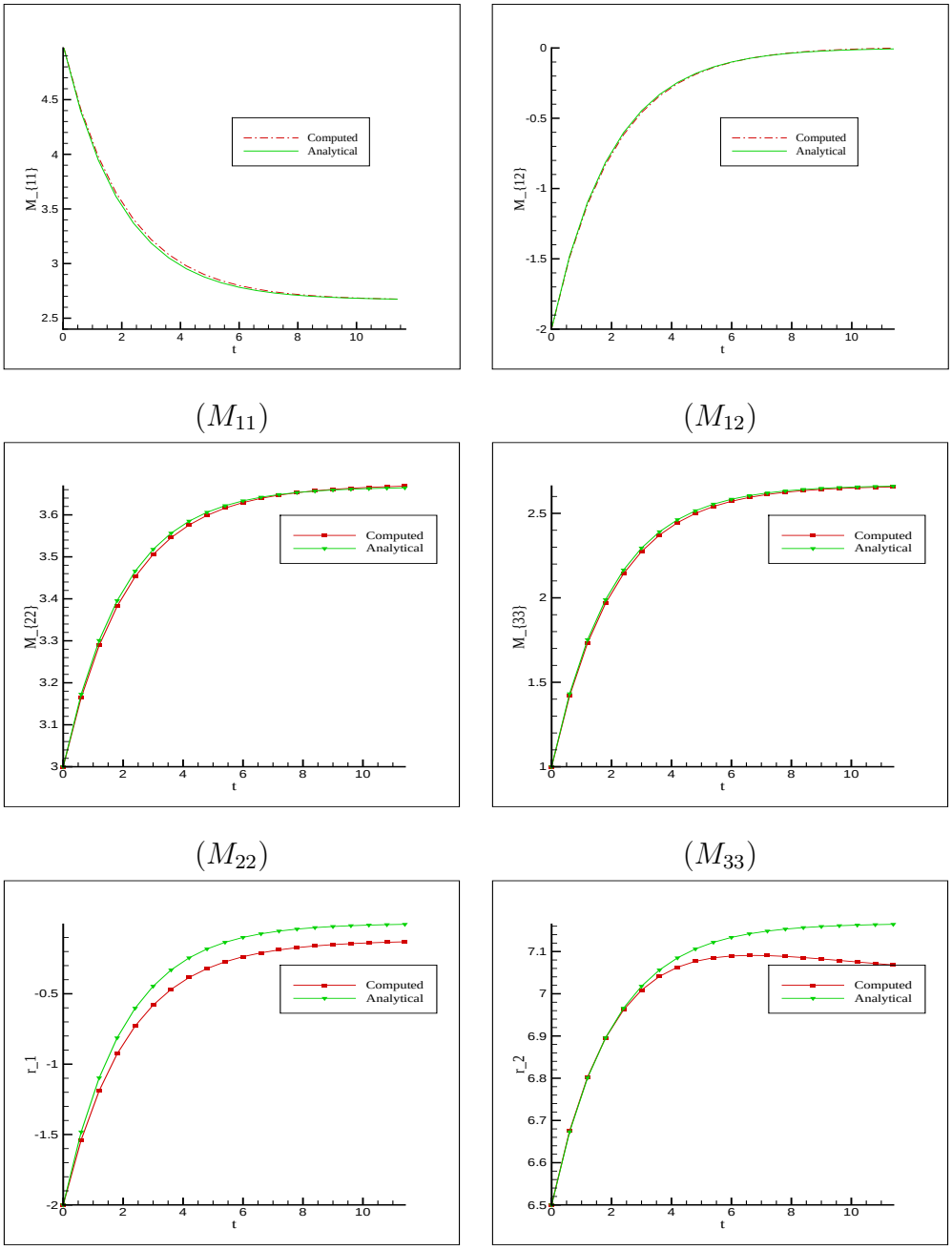

Fig. 2. Spectral-Lagrangian solver test for Maxwell type of elastic collisions constraining only mass, momentum and kinetic energy. Plot of higher order moments from (2.9): momentum flow $M_{11}, M_{12}, M_{22}, M_{33}$, energy flow r_1, r_2; N=16. Third order moments, such as the energy flow components, generate larger errors that are reduced by taking larger N.

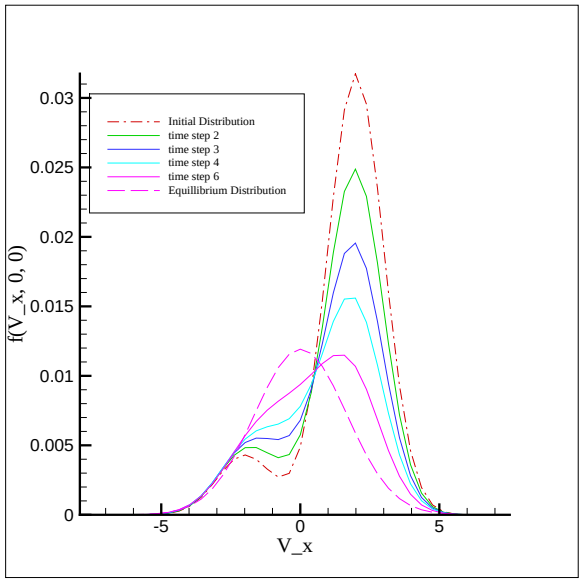

Fig. 3. Evolution of the distribution function for Maxwell type elastic collisions, N=40

5.2 Maxwell type of Elastic collisions - Bobylev-Krook-Wu (BKW) Solution

An explicit solution to the initial value problem (2.1) for elastic, Maxwell type of interactions ($\beta = 1, \lambda = 0$) was derived in [3] and later in [44] for initial states that have at least $2+\delta$-moments bounded. It is not of self-similar type, but it can be shown to converge to a Maxwellian distribution. This solution takes the form

$$f(v,t) = \frac{e^{-|v|^2/(2K\eta^2)}}{2(2\pi K\eta^2)^{3/2}}\left(\frac{5K-3}{K} + \frac{1-K}{K^2}\frac{|v|^2}{\eta^2}\right), \tag{5.1}$$

where $K = 1 - e^{-t/6}$ and η =initial distribution temperature. It is interesting to observe that this particular explicit solution is negative for small values of t. Consequently, in order to obtain an admissible probability distribution which may be assigned a physical meaning, f must be non-negative. This is indeed the case for any $K \geqslant \frac{3}{5}$ or $t \geqslant t_0 \equiv 6ln(\frac{5}{2}) \sim 5.498$.
This explicit solution formula is indeed an optimal tester to a homogeneous Boltzmann equation solver. We set the initial distribution function at $t = 0$ to be the BKW solution at $t = t_0$. The numerical approximation to the Boltzmann solver for this initial state and the exact evolution of the BKW solution are plotted for different values of N at various time steps in figure 4.

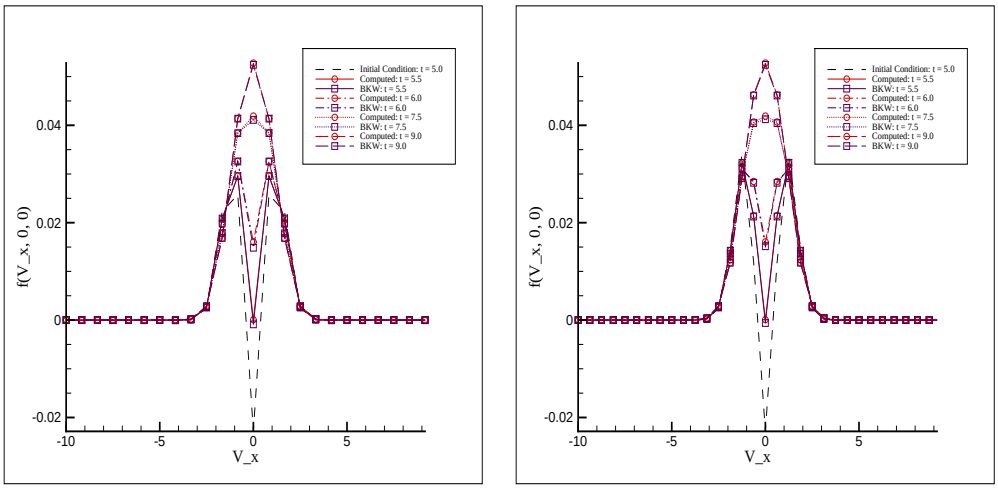

$(N = 24)$ $(N = 32)$

Fig. 4. BKW solution of the homogenous Boltzmann equation, ρ, and $\mathcal{E}(t)$ conserved

5.3 Hard Sphere Elastic Collisions

In (2.1), (2.2) or equivalently (2.4), we have $\beta = 1, J_\beta = 1$ and $\lambda = 1$ with the post-collisional velocities defined from (2.3). Unlike Maxwell type of interactions, there is no explicit expression for the moment equations and neither is there any explicit solution expression as in the BKW solution scenario. For hard sphere isotropic collisions, the expected behavior of the moments is similar to that of the Maxwell type of interactions case except that in this case, the moments somewhat evolve to the equilibrium a bit faster than in the former case i.e. figure 5. We also plot the time evolution of the distribution function starting from the convex combination of Maxwellians as described in a previous subsection in figure 6.

5.4 Inelastic Collisions

This is the case wherein the utility of the proposed method is the most clear. No other deterministic method can compute the distribution function in the case of inelastic collisions (isotropic). Our current method can compute a $3-D$ evolution without much complication and with exactly the same number of operations as used in an elastic collision case. This model works for all variable hard sphere interactions. Consider the special case of Maxwell ($\lambda = 0$) type of inelastic ($\beta \neq 1$) collisions in a space homogeneous Boltzmann Equation in (2.1), with (2.4) and (2.5). Let $\phi(v) = |v|^2$ be a smooth enough test function. Using the weak form of the Boltzmann equation with such a test function one can obtain the ODE governing the evolution of the kinetic energy $K(t) = \mathcal{E}(t)$

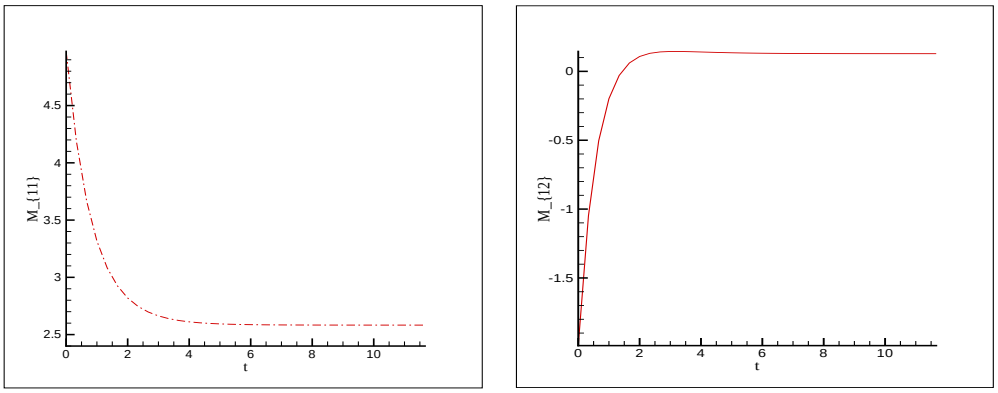

(M_{11})

(M_{12})

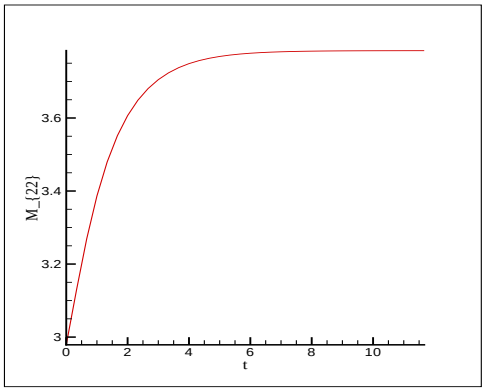

(M_{22})

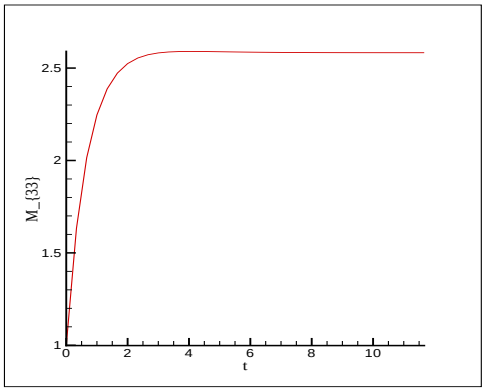

(M_{33})

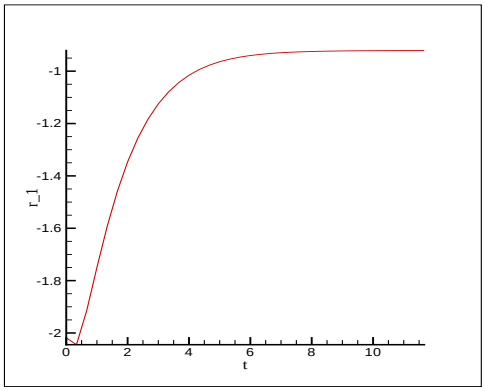

(r_1)

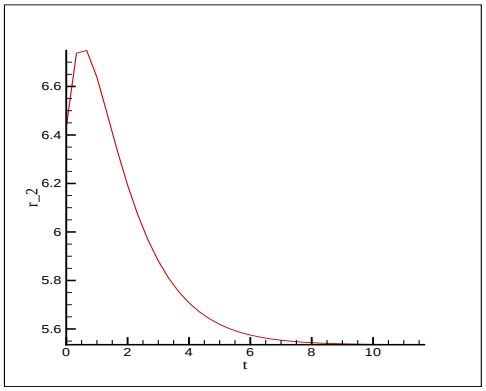

(r_2)

Fig. 5. Moments evolution for elastic hard sphere collisions: Momentum Flow $M_{11}, M_{12}, M_{22}, M_{33}$, Energy Flow r_1, r_2; N=16

(2.7):

$$K'(t) = \beta(1-\beta)(\frac{|V|^2}{2} - K(t))\,, \tag{5.2}$$

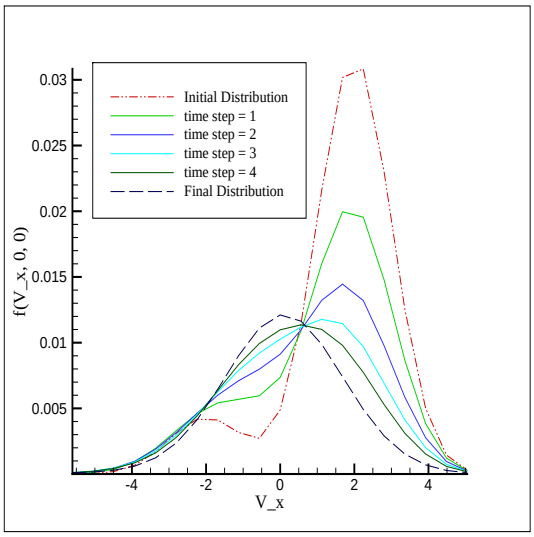

Fig. 6. Evolution of the distribution function for elastic hard sphere collisions; N = 32

where V - conserved (constant) bulk velocity of the distribution function. This gives the following solution for the kinetic energy as computed in (2.10)

$$K(t) = K(0)e^{-\beta(1-\beta)t} + \frac{|V|^2}{2}(1 - e^{-\beta(1-\beta)t}), \tag{5.3}$$

where $K(0)$ =kinetic energy at time $t = 0$. As we have an explicit expression for the kinetic energy evolving in time, this analytical moment can be compared with its numerical approximation for accuracy and the corresponding graph is given in figure 7. The general evolution of the distribution function in an inelastic collision environment is also shown in figure 7. In the conservation routine (constrained Lagrange multiplier method), energy is not used as a constraint and just density and momentum equations are used for constraints. Figure 7 shows the numerical accuracy of the method even though the energy (plotted quantity) is not being conserved as part of the constrained optimization method. So, the conservation correction with respect to density and momentum ensures that energy evolves as required and as expected. All simulations here, and those shown below, for inelastic interactions have been carried out for a value of the restitution coefficient $e = 0.5$, or equivalently $\beta = 0.75$.

5.5 Inelastic Collisions with Diffusion Term

We simulate next equations (2.11) and (2.12) modeling inelastic interactions in a randomly excited heat bath with constant temperature η. The evolution

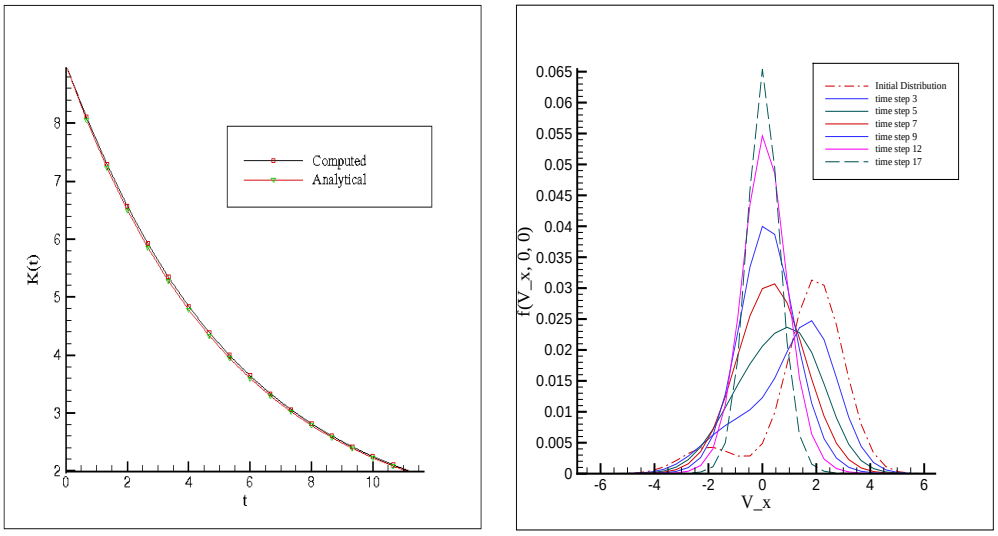

Fig. 7. Evolution of the Boltzmann equation for inelastic collisions of Maxwell type. Plots of the kinetic energy $\mathcal{E}(t)$ (left) and the probability distribution $f(v,t)$ (right); N=32

equation for the kinetic temperature as a function of time is given by:

$$\frac{dT}{dt} = 2\eta - \zeta\frac{1-e^2}{24}\int_{v\in\mathbb{R}^3}\int_{w\in\mathbb{R}^3}\int_{\sigma\in\mathbb{S}^2}(1-\mu)B(|u|,\mu)|u|^2 f(v)f(w)\,d\sigma dw dv\,. \tag{5.4}$$

In the case of inelastic Maxwell type interactions according to (2.10), the evolution of the temperature (5.4) has a closed form

$$\frac{dT}{dt} = 2\eta - \zeta\pi C_0(1-e^2)T\,, \tag{5.5}$$

which gives a closed expression for the time evolution of the kinetic temperature

$$T(t) = T_0 e^{-\zeta\pi C_0(1-e^2)t} + T_\infty^{MM}[1 - e^{-\zeta\pi C_0(1-e^2)t}]\,, \tag{5.6}$$

where

$$T_0 = \frac{1}{3}\int_{v\in\mathbb{R}^3}|v|^2 f(v)dv \qquad \text{and} \qquad T_\infty^{MM} = \frac{2\eta}{\zeta\pi C_0(1-e^2)}\,.$$

As it can be seen from the expression for T, in the absence of the diffusion term (i.e. $\eta = 0$) and for $e \neq 1$ (inelastic collisions), the kinetic temperature of the distribution function decays exponentially in time, just like in the previous section. So, inelastic interaction the presence of the diffusion term pushes the temperature to a positive stationary state $T_\infty^{MM} > 0$. Also note that if the interactions were elastic and the diffusion coefficient positive then, $T_\infty^{MM} = +\infty$, so the model would not admit stationary states with finite kinetic temperature. These properties were shown in [34] and similar time asymptotic behavior is expected in the case of hard sphere interactions where $T_\infty^{HS} > 0$ is shown to exist. However, the time evolution of the kinetic temperature is a non-local

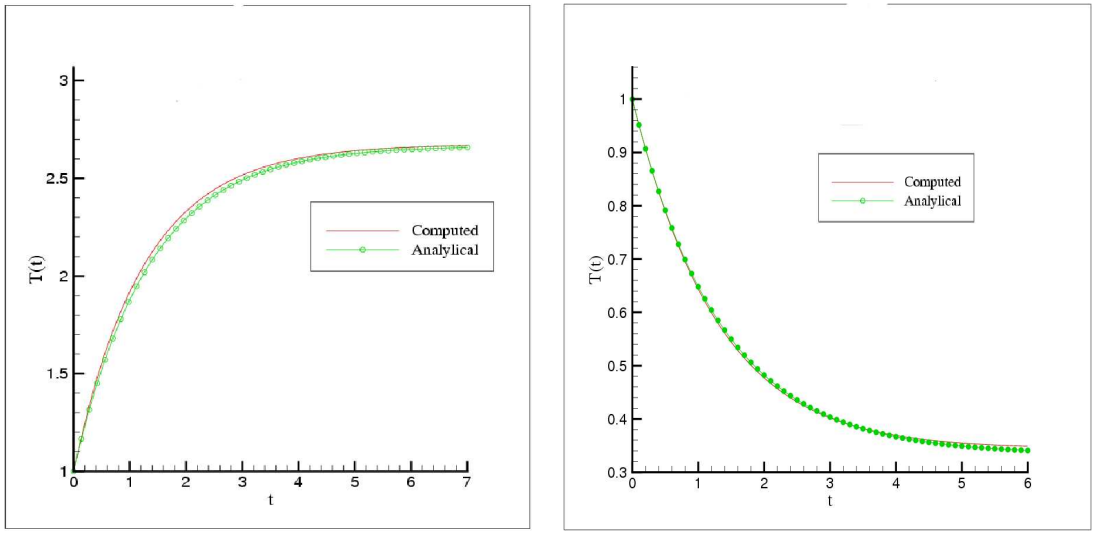

$(T_\infty^{MM} > T_0)$ $(T_\infty^{MM} < T_0)$

Fig. 8. Evolution of the kinetic temperature for inelastic collisions of Maxwell type with a diffusion term; N = 16.

integral (5.4) and does not satisfy a close ODE form (5.5).
We simulate both cases, hard spheres and Maxwell type inelastic interactions, choosing the diffusion parameter $\eta = 1$ and the inelasticity parameter $\beta = 0.75$. We also compared in figure 8, for the example of Maxwell type interactions, the kinetic temperature versus the exact analytical solution (5.6) for different initial data. In figure 9 observe the expected asymptotic behavior in the case of hard sphere inelastic interactions, for the same parameters values of η and β.
Notice that the conservation properties for this case of inelastic collisions with a diffusion term are set exactly like in the previous subsection (inelastic collisions without the diffusion term), i.e. we only constrain mass density an momentum.

5.6 Maxwell type of Elastic Collisions - Slow down process problem

We consider next the initial value problem (2.20) with $\beta = 1, J_\beta = 1$ and $B(|u|, \mu) = \frac{1}{4\pi}$, i.e. isotropic collisions. The second term is a linear collision integral modeling the effect of particle interactions and with a constant temperature thermostat which conserves only density, and the first term is the classical bilinear elastic collision integral from (2.20) conserving density, momentum and energy. The function $M(v)$ in (2.20) denotes the Maxwellian, given by $M_{\mathcal{T}}(v) = e^{\frac{-|v|^2}{(2\mathcal{T})}} \frac{1}{(2\pi\mathcal{T})^{3/2}}$, with $\mathcal{T}$ the constant thermostat temperature. In particular, it can be shown [14; 12] that any initial distribution function converges to the background distribution $M_{\mathcal{T}}$. This behavior is well captured

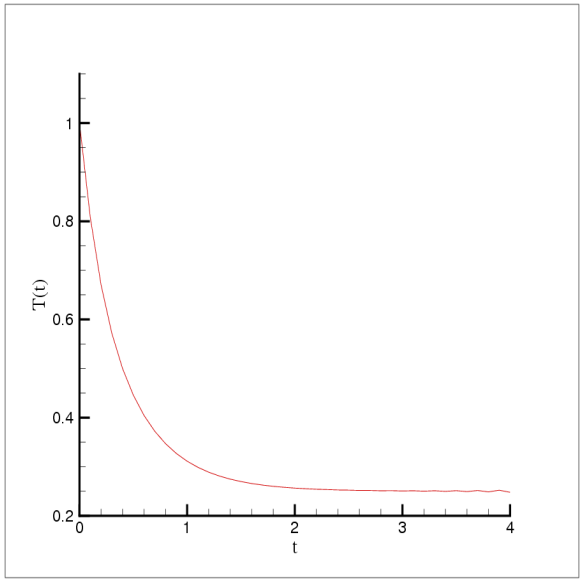

Fig. 9. Evolution of the kinetic temperature for inelastic, hard sphere collisions with a diffusion term and $T_\infty^{HS} < T_0$; N = 16.

by the numerical method. Indeed, figure 10 corresponds to an initial state of a convex combination of two Maxwellians. In addition, we can compute the long time approximation to the self-similar solution as follows. In the finite energy case of (4.6), with parameters for $p = 1, a = 1, \mu = \frac{2}{3}, \theta = \frac{4}{3}$ in (4.2), i.e. $p = 1$ in (4.15) and (4.16), the Fourier transform of self-similar solution takes the exact form

$$f_{\mathcal{T}}^{ss}(v,t) = \frac{\sqrt{(2)}}{\pi^{5/2}} \int_0^\infty \frac{1}{(1+s^2)^2} \frac{e^{-|v|^2/2\bar{T}}}{\bar{T}^{\frac{3}{2}}} ds \quad \bar{T} = \mathcal{T} + as^2 e^{\frac{-2t}{3}}\,, \tag{5.7}$$

As $t \to \infty$, the time rescaled numerical distribution is compared with the analytical solution $f_{\mathcal{T}}^{ss}$ for a positive background temperature $\mathcal{T}$ and it can be observed that converges to the Maxwellian $M_{\mathcal{T}}$. It can also be observed in figure 10, that the computed distribution is in very good agreement with the analytical self-similar distribution $f_{\mathcal{T}}^{ss}$ from (5.7). Similar agreement is observed for different constant values of $\mathcal{T}$ approaching 0 (figure 10).
The interesting asymptotics corresponding to power-like tails and infinitely many particles at zero energies occur only when $\mathcal{T} = 0$ as shown in (4.10). Since letting $\mathcal{T} = 0$ in the scheme created an instability, we proposed the following new strategy to counter this effect. We let instead $\mathcal{T} = \zeta e^{-\alpha t}$, ensuring that the thermostat temperature vanishes for large time, and set

$$\bar{T} = \zeta e^{-\alpha t} + a\, s^2 e^{\frac{-2t}{3}}\,, \tag{5.8}$$

where the role of α is very important and a proper choice needs to be made. In our simulations $a = 1$ and we take $\zeta = 0.25$ and the values of α need to be

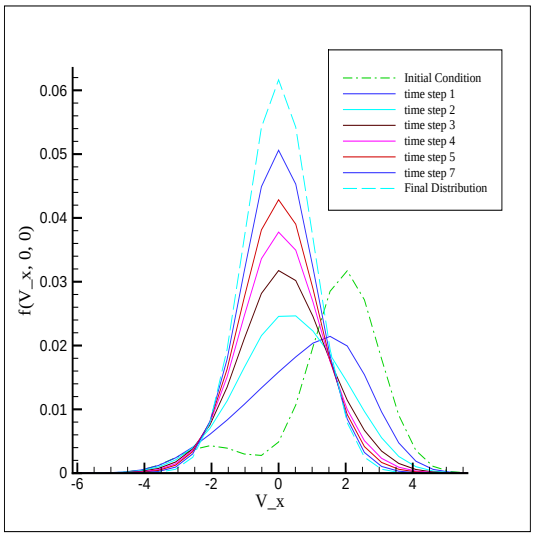

Evolving **pdf** $f(v,t)$

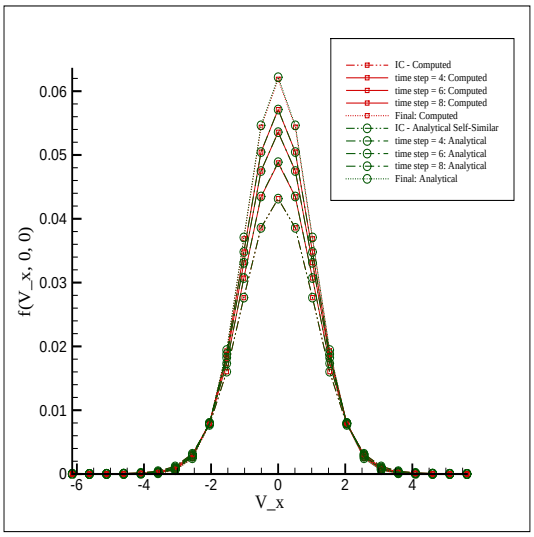

Computed **pdf** versus $f_{\mathcal{T}}^{ss}$ for $\mathcal{T} = 1$

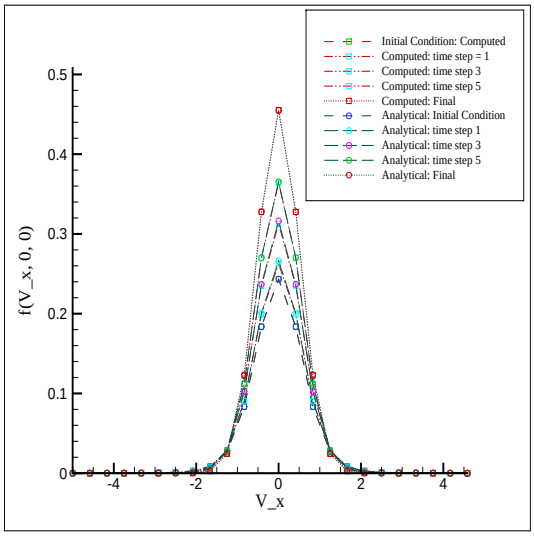

Computed **pdf** versus $f_{\mathcal{T}}^{ss}$ for $\mathcal{T} = 0.25$

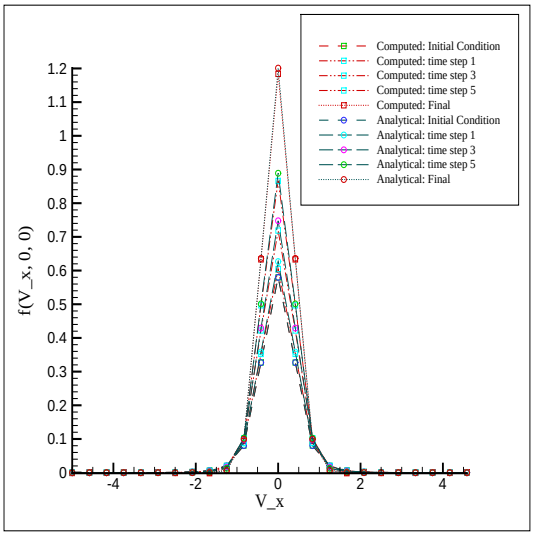

Computed **pdf** versus $f_{\mathcal{T}}^{ss}$ for $\mathcal{T} = 0.125$

Fig. 10. Evolution of the **pdf** of a slow down process for Maxwell type collisions with parameters $\Theta = 4/3, \mu = 2/3; N = 24$

chosen exactly as $\alpha = \mu(1) = 2/3$, the energy dissipation rate as described in section 4.2 to recover the asymptotics as in (4.10).

Remark: We notice that the procedure we use to compute approximations to self-similar solutions in free space to energy dissipative models of collisional Maxwell type uses time rescaling of the velocity by the inverse of the squared root of the kinetic energy (2.17), which it is, for a Maxwell type interaction model, exponential time rescaling in velocity space, and equivalently, in of Fourier modes. Such procedure may also be viewed as a non-uniform grid of Fourier modes that are distributed according to the continuum spectrum of the associated problem. This choice plays the equivalent role to the corresponding

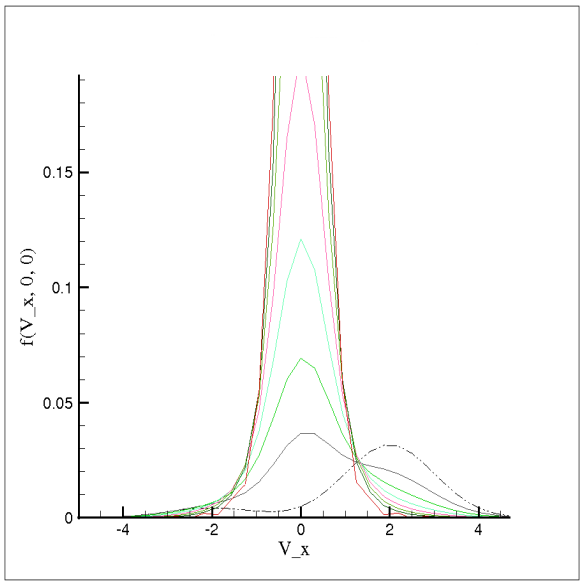

Fig. 11. Evolving **pdf** $f(v,t)$ for a slow down process for Maxwell type interactions with $\mathcal{T} = \frac{1}{4}e^{-2t/3}$, N = 32.

spectral approximation of the free space problem of the heat kernel, that is, the Green's function for the heat equation, which happens to be a similarity solution as well, due to the linearity of the problem in this case. In particular, we expect optimal algorithm complexity using such a non-equispaced Fast Fourier Transform, as obtained by Greengard and Lin [39] for spectral approximation of the free space heat kernel. This problem will be addressed in a forthcoming paper. The following plots elucidate the fact that the scheme can handle self-similar asymptotics to non-equilibrium states power-like high energy tails and blow up at the origin, which are achieved asymptotically with a decaying $\mathcal{T}$. For a decaying background temperature as in (5.8), figure 11 shows evolution of a convex combination of Maxwellians to a self-similar (blow up for zero energies and power-like for high energies) behavior. Figure 12 plots the computed distribution along with a Maxwellian with temperature equal to the computed temperature of the numerical solution. This illustrates that the computed approximation to the self-similar solution is largely deviated from a Maxwellian equilibrium. In order to better capture the power-like effect using this numerical method, we set $\mathcal{T} = \zeta e^{-2t/3} = \zeta e^{-\mu t}$, see (5.8), where $\mu = \mu(p)$ is related the spectral properties of the Fourier transformed equation as described in section 4.2 on the slow down process problem with $\mu = \mu(1)$ the energy dissipation rate. Thus, as it was computed in [14] and revised in section 4 of this paper, we know that for initial states with finite energy $p = 1$ and the corresponding energy dissipation rate is $\mu = \mu(1) = 2/3$. In particular $p_* = 1.5$ is the conjugate of $p = 1$ of the spectral curve m_q in Theorem 4.1 part (i). In addition, the rescaled probability will converge to the moments of

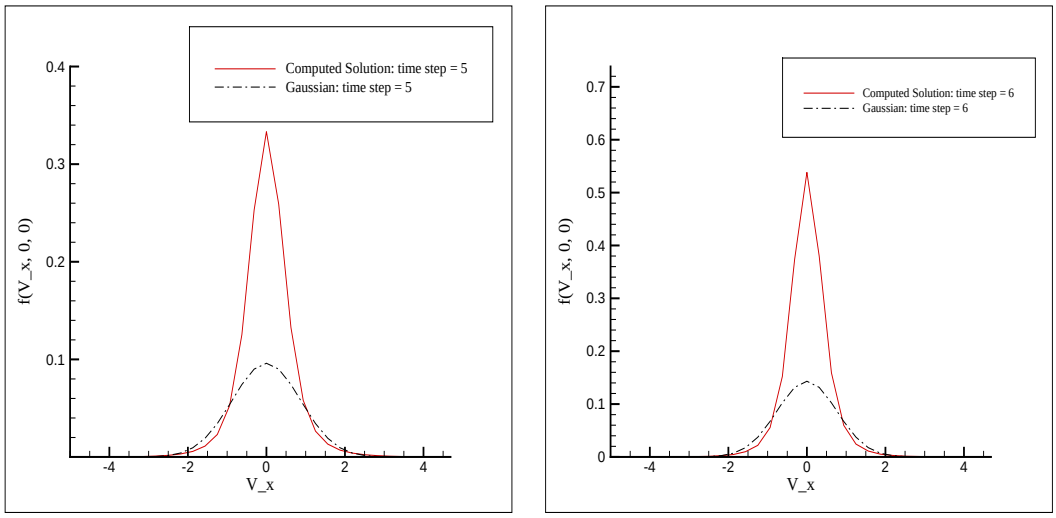

(time step = 5) (time step = 6)

Fig. 12. Computed **pdf** versus the Maxwellian distribution with kinetic temperature from the computed distribution, N=32.

the self-similar state (4.15), (4.16), that is

$$e^{-qt2/3}\int_{v\in\mathbb{R}^3} f(v)|v|^{2q}dv \to m_q\,,$$

and we know any moment m_q is unbounded for $q > p_* = 1.5$.
We have plotted in figure 13 the evolution of $e^{-qt2/3}\int_{v\in\mathbb{R}^3} f(v)|v|^{2q}dv$ for $q = 1, 1.3, 1.45, 1.5,\ 1.55, 1.7, 2.0$, computed for different values of $N = 10, 14, 16, 18, 22, 26$. It can be seen that, as time progresses and as the thermostat temperature $\mathcal{T}$ decreases to 0, the approximated numerically computed moments converge to $m_q, q \geq 1.5$ and start to become unbounded as predicted. The value $q = 1.5$ is the threshold value, as any moment $m_{q>1.5}(t) \to \infty$.
From the expected spectral accuracy analysis it can be observed the numerical $m_{q>1.5}(t)$ moments improve the growth zone for larger final times as the value of N increases. The reason for such an effect is because the velocity domain is truncated and we use only a finite number of Fourier modes. That makes the computed distribution function to take small negative values for large velocities contributing to numerical errors that may cause m_q to peak and then relax back. In particular, larger order moments of the computed self-similar asymptotics with the negative oscillating parts on large energy tails, result in large negative moment values for the above mentioned values of N creating large negative errors. However it is noticed that the negative oscillation values of $f(t, v)$ coincide with large velocity values used in getting approximating m_q moments, for $q > 1.5$, and that such an error is reduced in time for larger number N of of Fourier modes. Finally we point out that a FFTW package has been used. We have noticed in our numerics are not reliable for that for the specific choice of values $N \neq 6, 10, 14, 18, 22, 26, ..., 6+4k; k = 0, 1, 2, 3, ...$
More precisely, the approximating moments to $m_q(t)$ start to take negative

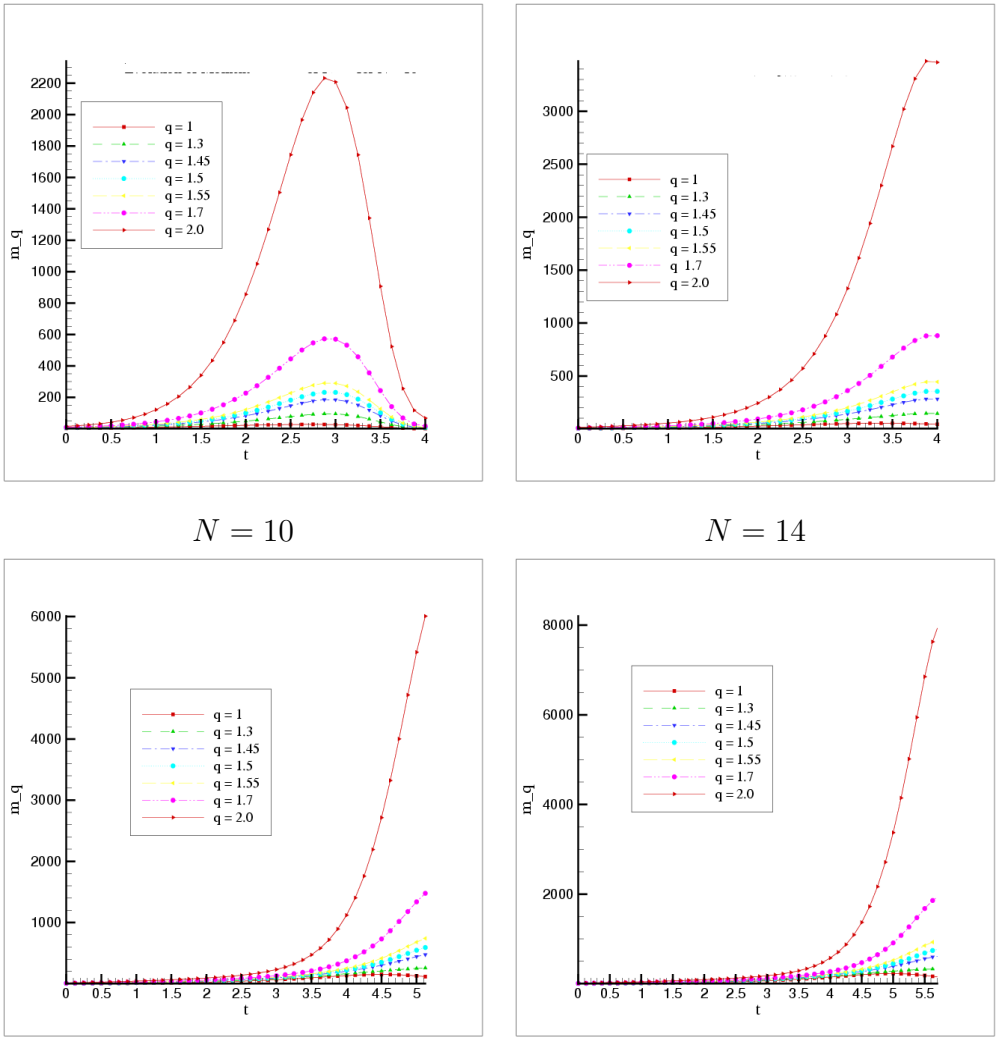

Fig. 13. $m_q(t)$ for $\mathcal{T} = e^{-2t/3}$

values very quickly, as seen in figure 14 for $N = 16$ and $N = 20$, making the numerical solution inadmissible since analytically $m_q(t) > 0, \forall t$. Such effect may be due to the particular choice of the FTTW solver.

6 Conclusions and Future Work

In conclusion, the presented numerical method works for elastic and inelastic variable hard sphere interactions. This is first of its kind as no additional modification is required to compute for elastic and inelastic collisions. In comparison with the known analytical results (moment equations for elastic BTE, BKW self-similar solution, attracting Bobylev-Cercignani-Gamba self-similar solutions for elastic collisions in a slow down process), the computed results

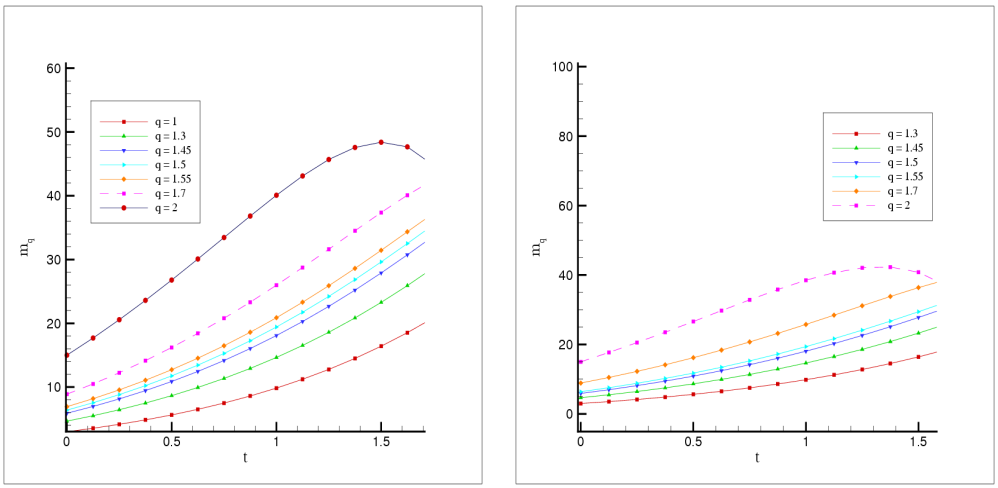

$N = 16$ $N = 20$

Fig. 14. $m_q(t)$ for $\mathcal{T} = e^{-2t/3}$

.

are found to be very accurate. The method employs a Fast Fourier Transform for faster evaluation of the collision integral. Even though the method is implemented for a uniform grid in velocity space, it can even be implemented for a non-uniform velocity grid. The only challenge in this case is computing the Fast Fourier Transform on such a non-uniform grid. There are available packages for this purpose, but such a non-uniform FFT can also be implemented using a high degree polynomial interpolation and this possibility is currently being explored. The integration over the unit sphere is avoided completely and only a simple integration over a regular velocity grid is needed. Even though a trapezoidal rule is used as an integration rule, other integration rules like a Gaussian quadrature can be used to get better accuracy. For time discretization, a simple second-order Runge Kutta scheme is used. The proposed method has a big advantage over other non-deterministic methods as the exact distribution function can actually be computed instead of just the averages.

Implementation of this scheme for the space inhomogeneous case is currently developed by the authors by means of splitting algorithms in advection and collision components. Next step in this direction would be to implement the method for a practical 1 and $2-D$ space inhomogeneous problems such shock tube phenomena for specular and diffusive boundary conditions, resolution of the probability distribution function boundary layer discontinuity for diffusive boundary conditions with a sudden change of boundary temperature, and Rayleigh-Benard instability or a Couette flow problem.

7 Acknowledgements

The authors would like to thank Sergej Rjasanow for discussions about the conservation properties of the numerical method and for other comments. Both authors are partially supported under the NSF grant DMS-0507038. Support from the Institute of Computational Engineering and Sciences and the University of Texas Austin is also gratefully acknowledged.

References

[1] R. J. Alonso, I. M. Gamba, Propagation of l^1 and l^∞ Maxwellian weighted bounds for derivatives of solutions to the homogeneous elastic Boltzmann equation, To appear in Journal of Mathematiques Pures et Appliquées. URL http://arxiv.org/abs/0710.5256

[2] G. A. Bird, Molecular Gas Dynamics, Clarendon Press, Oxford, 1994.

[3] A. V. Bobylev, Exact solutions of the Boltzmann equation, (Russian) Dokl. Akad. Nauk SSSR 225 (1975) 1296–1299.

[4] A. V. Bobylev, Exact solutions of the nonlinear Boltzmann equation and the theory of relaxation of a Maxwellian gas, Translated from Teoreticheskaya i Mathematicheskaya Fizika 60 (1984) 280 – 310.

[5] A. V. Bobylev, The theory of the nonlinear spatially uniform Boltzmann equation for Maxwell molecules, Mathematical physics reviews; Soviet Sci. Rev. Sect. C Math. Phys. Rev. 7 (1988) 111–233.

[6] A. V. Bobylev, J. A. Carrillo, I. M. Gamba, On some properties of kinetic and hydrodynamic equations for inelastic interactions, Journal of Statistical Physics 98 (2000) 743–773.

[7] A. V. Bobylev, C. Cercignani, Discrete velocity models without nonphysical invariants, Journal of Statistical Physics 97 (1999) 677–686.

[8] A. V. Bobylev, C. Cercignani, Exact eternal solutions of the Boltzmann equation, Journal of Statistical Physics 106 (2002) 1019–1038.

[9] A. V. Bobylev, C. Cercignani, The inverse laplace transform of some analytic functions with an application to the eternal solutions of the Boltzmann equation, Applied Mathematics Letters 15 (2002) 807–813(7).

[10] A. V. Bobylev, C. Cercignani, Moment equations for a granular material in a thermal bath, Journal of Statistical Physics 106 (2002) 547–567(21).

[11] A. V. Bobylev, C. Cercignani, Self-similar asymptotics for the Boltzmann equation with inleastic and elastic interactions, Journal of Statistical Physics 110 (2003) 333–375.

[12] A. V. Bobylev, C. Cercignani, I. M. Gamba, On the self-similar asymptotics for generalized non-linear kinetic Maxwell models, to appear in Communication in Mathematical Physics.
URL http://arxiv.org/abs/math-ph/0608035

[13] A. V. Bobylev, C. Cercignani, G. Toscani, Proof of an asymptotic property of self-similar solutions of the Boltzmann equation for granular materials, Journal of Statistical Physics 111 (2003) 403–417.

[14] A. V. Bobylev, I. M. Gamba, Boltzmann equations for mixtures of Maxwell gases: Exact solutions and power like tails, Journal of Statistical Physics 124 (2006) 497–516.

[15] A. V. Bobylev, I. M. Gamba, V. Panferov, Moment inequalities and high-energy tails for Boltzmann equations with inelastic interactions, Journal of Statistical Physics 116 (2004) 1651–1682.

[16] A. V. Bobylev, M. Groppi, G. Spiga, Approximate solutions to the problem of stationary shear flow of smooth granular materials, Eur. J. Mech. B Fluids 21 (2002) 91–103.

[17] A. V. Bobylev, S. Rjasanow, Difference scheme for the Boltzmann equation based on the fast fourier transform, European journal of mechanics. B, Fluids 16:22 (1997) 293–306.

[18] A. V. Bobylev, S. Rjasanow, Fast deterministic method of solving the Boltzmann equation for hard spheres, European journal of mechanics. B, Fluids 18:55 (1999) 869–887.

[19] A. V. Bobylev, S. Rjasanow, Numerical solution of the Boltzmann equation using fully conservative difference scheme based on the fast fourier transform, Transport Theory Statist. Phys. 29 (2000) 289–310.

[20] J. E. Broadwell, Study of rarefied shear flow by the discrete velocity method, J. Fluid Mech. 19 (1964) 401–414.

[21] H. Cabannes, Global solution of the initial value problem for the discrete Boltzmann equation, Arch. Mech. (Arch. Mech. Stos.) 30 (1978) 359–366.

[22] C. Cercignani, Recent developments in the mechanics of granular materials, Fisica matematica e ingegneria delle strutture, Bologna: Pitagora Editrice (1995) 119–132.

[23] C. Cercignani, Shear flow of a granular material, Journal of Statistical Physics 102 (2001) 1407–1415.

[24] C. Cercignani, H. Cornille, Shock waves for a discrete velocity gas mixture, Journal of Statistical Physics 99 (2000) 115–140.

[25] M. H. Ernst, R. Brito, Driven inelastic Maxwell models with high energy tails, Phys. Rev. E 65 (4) (2002) 040301.

[26] M. H. Ernst, R. Brito, Scaling solutions of inelastic Boltzmann equations with over-populated high energy tails, Journal of Statistical Physics 109 (2002) 407–432.

[27] F. Filbet, C. Mouhot, L. Pareschi, Solving the Boltzmann equation in nlogn, SIAM J. Sci. Comput. 28 (2006) 1029–1053.

[28] F. Filbet, G. Russo, High order numerical methods for the space non homogeneous Boltzmann equation, Journal of Computational Physics 186 (2003) 457–480.

[29] F. Filbet, G. Russo, High order numerical methods for the space non homogeneous Boltzmann equation, Journal of Computational Physics 186 (2003) 457 – 480.

[30] N. Fournier, S. Mischler, A Boltzmann equation for elastic, inelastic and coalescing collisions, Journal de mathematiques pures et appliques 84 (2005) 1173–1234.

[31] M. Frigo, S. G. Johnson, Fast fourier transform of the west.
URL `www.fftw.org`

[32] E. Gabetta, L. Pareschi, G. Toscani, Relaxation schemes for nonlinear kinetic equations, SIAM J. Numer. Anal. 34 (1997) 2168–2194.

[33] I. M. Gamba, V. Panferov, C. Villani, Upper Maxwellian bounds for the spatially homogeneous Boltzmann equation, To appear in Arch.Rat.Mec.Anal.
URL `http://arxiv.org/abs/math/0701081`

[34] I. M. Gamba, V. Panferov, C. Villani, On the Boltzmann equation for diffusively excited granular media, Communications in Mathematical Physics 246 (2004) 503–541(39).

[35] I. M. Gamba, S. Rjasanow, W. Wagner, Direct simulation of the uniformly heated granular Boltzmann equation, Mathematical and Computer Modelling 42 (2005) 683–700.

[36] I. M. Gamba, S. H. Tharkabhushanam, Convergence and error analysis of spectral-Lagrange Boltzmann solver, In preparation.

[37] I. M. Gamba, S. H. Tharkabhushanam, Spectral lagragian solvers for boundary value problems for the Boltzmann Transport Equation for rarefied, monoatomic, In preparation.

[38] R. L. Greenblatt, J. L. Lebowitz, Product measure steady states of generalized zero range processes, J. Phys. A 39 (2006) 1565–1573.

[39] L. Greengard, P. Lin, Spectral approximation of the free-space heat kernel, Appl. Comput. Harmon. Anal. 9 (1) (2000) 83–97.

[40] M. Herty, L. Pareschi, M. Seaid, Discrete-velocity models and relaxation schemes for traffic flows, SIAM J. Sci. Comput. 28 (2006) 1582–1596.

[41] I. Ibragimov, S. Rjasanow, Numerical solution of the Boltzmann equation on the uniform grid, Computing 69 (2002) 163–186.

[42] R. Illner, On the derivation of the time-dependent equations of motion for an ideal gas with discrete velocity distribution, J. de Mecanique 17 (1978) 781–796.

[43] S. Kawashima, Global solution of the initial value problem for a discrete velocity model of the Boltzmann equation, Proc. Japan Acad. Ser. A Math. Sci. 57 (1981) 19–24.

[44] K. Max, W. T. Tsun, Formation of Maxwellian tails, Physical Review Letters 36 (1976) 1107–1109.

[45] L. Mieussens, Discrete-velocity models and numerical schemes for the Boltzmann-bgk equation in plane and axisymmetric geometries, Journal of Computational Physics 162 (2000) 429–466.

[46] J. M. Montanero, A. Santos, Computer simulation of uniformly heated granular fluids, Gran. Matt. 2 (2000) 53–64.

[47] S. J. Moon, M. D. Shattuck, J. Swift, Velocity distributions and correlations in homogeneously heated granular media, Physical Review E 64

(2001) 031303.
[48] C. Mouhot, L. Pareschi, Fast algorithms for computing the Boltzmann collision operator, Math. Comp. 75 (2006) 1833–1852.
[49] K. Nanbu, Direct simulation scheme derived from the Boltzmann equation i.monocomponent gases, J. Phys. Soc. Japan 52 (1983) 2042 – 2049.
[50] T. V. Noije, M. Ernst, Velocity distributions in homogeneously cooling and heated granular fluids, Gran. Matt. 1:57(1998).
[51] V. Panferov, S. Rjasanow, Deterministic approximation of the inelastic Boltzmann equation, Unpublished manuscript.
[52] L. Pareschi, B. Perthame, A fourier spectral method for homogenous Boltzmann equations, Transport Theory Statist. Phys. 25 (2002) 369–382.
[53] L. Pareschi, G. Russo, Numerical solution of the Boltzmann equation. i. spectrally accurate approximation of the collision operator, SIAM J. Numerical Anal. (Online) 37 (2000) 1217–1245.
[54] L. Pareschi, G. Toscani, Self-similarity and power-like tails in nonconservative kinetic models, J. Stat. Phys. 124 (2006) 747–779.
[55] S. Rjasanow, W. Wagner, A stochastic weighted particle method for the Boltzmann equation, Journal of Computational Physics (1996) 243–253.
[56] S. Rjasanow, W. Wagner, Stochastic Numerics for the Boltzmann Equation, Springer, Berlin, 2005.
[57] C. Villani, Handbook of Fluid dynamics, chap. A Review of Mathematical Topics in Collisional Kinetic Theory, Elsevier, 2003, pp. 71–306.
URL `http://www.umpa.ens-lyon.fr/ cvillani`
[58] W. Wagner, A convergence proof for bird's direct simulation monte carlo method for the Boltzmann equation, Journal of Statistical Physics (1992) 1011–1044.
[59] D. R. M. Williams, F. MacKintosh, Driven granular media in one dimension: Correlations and equation of state, Phys. Rev. E 54 (1996) 9–12.
[60] Y. Zheng, H. Struchtrup, A linearization of mieussens's discrete velocity model for kinetic equations, Eur. J. Mech. B Fluids 26 (2007) 182–192.